

4-1-2004

Characterization Of Cadmium Zinc Telluride Films And Solar Cells On Glass And Flexible Substrates By RF Sputtering

Jagadish Gaduputi
University of South Florida

Follow this and additional works at: <https://digitalcommons.usf.edu/etd>



Part of the [American Studies Commons](#)

Scholar Commons Citation

Gaduputi, Jagadish, "Characterization Of Cadmium Zinc Telluride Films And Solar Cells On Glass And Flexible Substrates By RF Sputtering" (2004). *USF Tampa Graduate Theses and Dissertations*.
<https://digitalcommons.usf.edu/etd/1041>

This Thesis is brought to you for free and open access by the USF Graduate Theses and Dissertations at Digital Commons @ University of South Florida. It has been accepted for inclusion in USF Tampa Graduate Theses and Dissertations by an authorized administrator of Digital Commons @ University of South Florida. For more information, please contact digitalcommons@usf.edu.

Characterization Of Cadmium Zinc Telluride Films And Solar Cells On Glass And
Flexible Substrates By RF Sputtering

by

Jagadish Gaduputi

A thesis submitted in partial fulfillment
of the requirements for the degree of
Master of Science in Electrical Engineering
Department of Electrical Engineering
College of Engineering
University of South Florida

Major Professor: Christos S.Ferekides, Ph.D.
Don L.Morel, Ph.D.
Yun.L.Chiou, Ph.D.

Date of Approval:
April 1, 2004

Keywords: polyimide, czt, tandem devices, photovoltaics .

© Copyright 2004 , Jagadish Gaduputi

DEDICATION

This work is dedicated to my family.

ACKNOWLEDGMENTS

I would like to thank my Major Professor, Dr.Christos S. Ferekides, for his guidance and support during the course of this work. He has been a great source of inspiration during my time at Clean Energy Research Center and will remain so in future. I would like to thank Dr.Don L. Morel and Dr.Yun L. Chiou for their guidance in the fulfillment of this thesis. I would like to thank my colleague and all my friends for their support during this work.

TABLE OF CONTENTS

LIST OF TABLES	iv
LIST OF FIGURES	v
ABSTRACT	viii
CHAPTER 1.INTRODUCTION	1
1.1 The Path to Renewable Energy	1
1.2 Photovoltaics-An Overview of Progress	2
1.3 Beyond Single Crystal Silicon	4
CHAPTER 2.THEORY OF SOLAR CELLS	7
2.1 Solar Power	7
2.2 Solar Cell Parameters	8
CHAPTER 3.LITERATURE REVIEW	12
3.1 Why Tandem?	12
3.2 MBE Grown $Cd_{1-x}Zn_xTe$ Solar Cells	14
3.3 Effect of Pre-contact Treatments on $Cd_{1-x}Zn_xTe$ Films	16
3.4 Contact Technology	17

3.5 Thin Films on Flexible Polyimide Substrates	18
CHAPTER 4.PROCESSING	21
4.1 Cell Structure	21
4.2 DepositionTechnique	22
4.2.1 Transparent Conducting Oxides	22
4.2.2 Window Layer	22
4.2.3 Cadmium Zinc Telluride	23
4.2.4 Back Contact	24
4.3 Measurements	24
4.3.1 Spectral Response	24
4.3.2 I-V	25
4.3.3 SEM and XRD	25
CHAPTER 5.RESULTS AND DISCUSSION	26
5.1 CZT Material Properties	26
5.1.1 Optical Properties	26
5.1.2 Structural Properties	27
5.2 CZT Solar Cells	30
5.2.1 Effect of N ₂ on CZT Device Performance	30
5.2.2 ITO/ZnSe/CZT	33
5.2.3 SnO ₂ /CZTand SnO ₂ /CdS/CZT	35
5.2.4 ZnTe Contact	40
5.2.5 Post Deposition Treatment on CZT Films	42
5.3 CZT Thin Films on Flexible Polyimide Substrates	44

5.3.1 Effect of Temperature on Polyimide Substrate	44
5.3.2 TCO Deposition on Polyimide	45
5.3.3 CZT Films on Polyimide	46
CHAPTER 6.CONCLUSIONS	50
REFERENCES	52

LIST OF TABLES

Table 1. Conditions and Results of 15 Minute Pre-contact Treatments on CZT	16
Table 2. Calibrated Substrate Temperatures	24
Table 3. Comparison of As Deposited and Annealed CZT Devices on SnO ₂ and SnO ₂ /CdS Substrates	36

LIST OF FIGURES

Figure 1. World Energy Related Carbon Dioxide Emissions,1970-2020	2
Figure 2. PV Roadmap Goal	4
Figure 3. Best Laboratory Cell Efficiencies for Thin Films	5
Figure 4. Solar Spectrum	7
Figure 5. Equivalent Circuit of a Solar Cell	9
Figure 6. Dark and Light I-V Characteristics of a Solar Cell	10
Figure 7. Contour Map of Conversion Efficiency of a Tandem Device	13
Figure 8. Four-Terminal Tandem Solar Cell Structure	14
Figure 9. XRD of MBE Grown CZT	15
Figure 10. SR of n-p and n-i-p CZT Solar Cells	15
Figure 11. XRD(Left) and Transmission(Right) of ITO on Polyimide and Glass	19
Figure 12. SEM of As Deposited(Left) and CdCl ₂ Treated(Right) CdTe\CdS\TCO\Poly	20
Figure 13. I-V Characteristics of CdTe Solar Cell on Polyimide	20
Figure 14. CZT Solar Cell Structure on Glass(Top) and Flexible Polyimide Substrate(Bottom)	21
Figure 15. Co-sputtering Chamber for CZT Deposition	23
Figure 16. Optical Transmission of CZT	26
Figure 17. Measured Bandgap of CZT	27
Figure 18. XRD of As Deposited and Annealed CZT Films	28

Figure 19. SEM of As Deposited(Top) and Annealed(Bottom) CZT Films on Glass/SnO ₂ Substrate	29
Figure 20. Effect of N ₂ on V _{oc} and J _{sc} for As Deposited SnO ₂ /CZT Solar Cells	31
Figure 21. Effect of N ₂ on V _{oc} and J _{sc} for Annealed SnO ₂ /CZT Solar Cells	31
Figure 22. Effect of N ₂ on V _{oc} and J _{sc} for As Deposited SnO ₂ /CdS/CZT Solar Cells	32
Figure 23. Effect of N ₂ on V _{oc} and J _{sc} for Annealed SnO ₂ /CdS/CZT Solar Cells	32
Figure 24. Effect of Annealing on ITO/ZnSe/CZT Solar Cells	34
Figure 25. Spectral Response of Annealed ITO/ZnSe/CZT Devices	35
Figure 26. J-V Data for As Deposited SnO ₂ /CZT Solar Cells	37
Figure 27. J-V Data for Annealed SnO ₂ /CZT Solar Cells	37
Figure 28. J-V Data for As Deposited SnO ₂ /CdS/CZT Solar Cells	38
Figure 29. J-V Data for Annealed SnO ₂ /CdS/CZT Solar Cells	38
Figure 30. Spectral Response of As Deposited and Annealed SnO ₂ /CZT Solar Cells	39
Figure 31. Spectral Response of As Deposited and Annealed SnO ₂ /CdS/CZT Solar Cells	39
Figure 32. J-V Data for As Deposited SnO ₂ /CdS/CZT/ZnTe Solar Cells	40
Figure 33. J-V Data for Annealed SnO ₂ /CdS/CZT/ZnTe Solar Cells	41
Figure 34. Spectral Response of As Deposited SnO ₂ /CdS/CZT/ZnTe Solar Cells	41
Figure 35. Spectral Response of Annealed SnO ₂ /CdS/CZT/ZnTe Solar Cells	42
Figure 36. Transmission of Unprocessed and Annealed Polyimide Substrate	45
Figure 37. Transmission of ITO, ITO/ZnO and ITO/SnO ₂ Films on Polyimide	46
Figure 38. XRD of CZT on Polyimide	47

Figure 39. SEM Images of CZT Deposited at 250 °C(Top) and 300 °C(Bottom) on Polyimide Substrate

48

CHARACTERIZATION OF CADMIUM ZINC TELLURIDE FILMS AND SOLAR CELLS ON GLASS AND FLEXIBLE SUBSTRATES BY RF SPUTTERING

Jagadish Gaduputi

ABSTRACT

High performance multijunction solar cells based on polycrystalline thin films will require a wide bandgap top cell with at least 15% efficiency. With the bottom cell being CIGS which have already demonstrated the required efficiencies, this work aims to study the complete fabrication and performance of $\text{Cd}_{1-x}\text{Zn}_x\text{Te}$ solar cells with a bandgap of 1.7eV on glass and flexible polyimide substrates.

$\text{Cd}_{1-x}\text{Zn}_x\text{Te}$ films were deposited by RF magnetron co-sputtering with CdTe and ZnTe sources. By varying the composition of $\text{Cd}_{1-x}\text{Zn}_x\text{Te}$ being deposited the required bandgap of 1.7eV was achieved. The optical and structural properties of the films were studied with optical transmission, SEM and XRD measurements. The films exhibited high optical transmission and pinhole free grain structure. CZT solar cells were fabricated on glass and flexible polyimide substrate and were analyzed by J-V and spectral response measurements. The effect of post deposition treatments and the effect of N_2 during sputtering on CZT device performance were studied.

CHAPTER 1

INTRODUCTION

1.1 The Path To Renewable Energy

As the demand for more electric power increases, the need for an environmentally benign means of producing electricity becomes very important. Today fossil fuels are the primary source to heat, power homes and fuel our cars. It is convenient to use coal, oil, and natural gas for meeting our energy needs, but we have limited supply of these fuels on earth. Sooner or later these currently used power plants will be replaced with renewable energy sources. According to recent predictions the permanent decline in the global oil production rate is expected to start within the next 10-20 years. World-wide oil prices will then rise considerably, favoring the introduction of various renewable energy sources such as the direct conversion of the sunlight into electrical energy using solar cells and other renewable power sources like hydroelectric, wind or geothermal power conversion systems [2].

Even if we had unlimited supply of fossil fuels, using renewable energy is better for the environment as renewable energy technologies are clean and green. Burning fossil fuels sends greenhouse gases into the atmosphere, trapping the sun's heat and contributing to global warming.

About 20,000 million tons of carbon dioxide is delivered into the atmosphere every year, mainly by burning fossil fuels. Today's plants are unable to absorb this huge amount of

CO₂. As a result the CO₂ concentration in the atmosphere has continued to mount since the industrial revolution as shown in figure 1 [1]. This has added to the greenhouse effect considerably and will increase the global mean surface temperature by another 1 to 5.0 degrees by the year 2100 depending on future emissions and the actual climate sensitivity. This temperature change has already increased the frequency and severity of natural disasters and are likely to have more severe effects for humans and other life

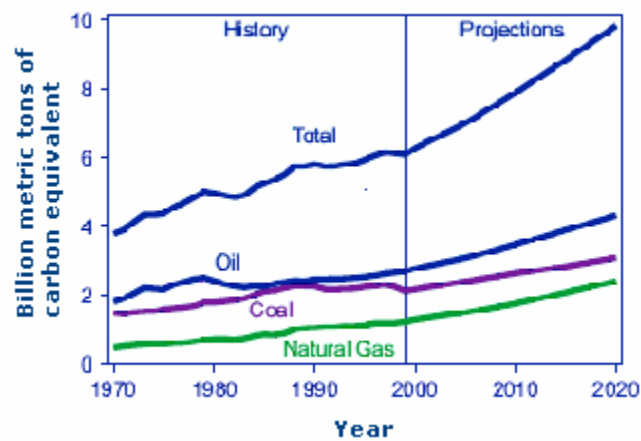


Figure 1. World Energy Related Carbon Dioxide Emissions

By Fuel Type, 1970-2020

forms on Earth within the next few decades. Fortunately we have renewable energy sources like solar energy which neither run out nor have significant harmful effects on our environment.

1.2 Photovoltaics-An Overview of Progress

The term photovoltaic is derived by combining the greek word for light, photos, with volt, the name of the unit of electromotive force. The term photovoltaic therefore signifies the generation of electricity from light. The discovery of Photovoltaic effect is generally credited to French physicist Edmond Becquerel in 1839, but it remained a curiosity of

science for the next three quarters of century. Bequeral found that certain materials would produce small amounts of electric currents when exposed to light. The effect was first studied in solids, such as selenium, by Heinrich Hertz in 1870s. Soon afterward selenium photovoltaic cells were converting light to electricity at 1% to 2% efficiency. Selenium was quickly adopted into emerging field of photography for use in light measuring devices [2].

Major steps toward commercializing PV were taken in the 1940s and early 1950s when the Czochralski process for producing highly pure crystalline silicon was developed. In 1954, scientists at bell laboratories depended on the Czochralski process to develop the first crystalline silicon photovoltaic cell, which had an efficiency of 4% [2].

Although a few attempts were made in the 1950s to use silicon solar cells in commercial products, it was the new space program that gave the technology its first major application. In 1958 the US Vanguard space satellite carried a small array of PV cells to power its radio, the cell worked so well that PV technology has been part of space program ever since. Today solar cells power virtually all satellites, including those used for communication satellites, defense and scientific research. Despite these advances, PV in 1970 was still too expensive for most terrestrial uses. In the mid 70s rising energy costs sparked by a world oil crisis renewed interest in making PV technology more affordable. Since then government, industry and research organizations have invested hundred of millions of dollars in research, development and production. Much of this effort has gone in the development of crystalline silicon the material bell scientists used to make the first solar cells. As a result crystalline silicon have become more and more efficient, reliable and durable. Today's commercial PV systems can convert from 10-15%

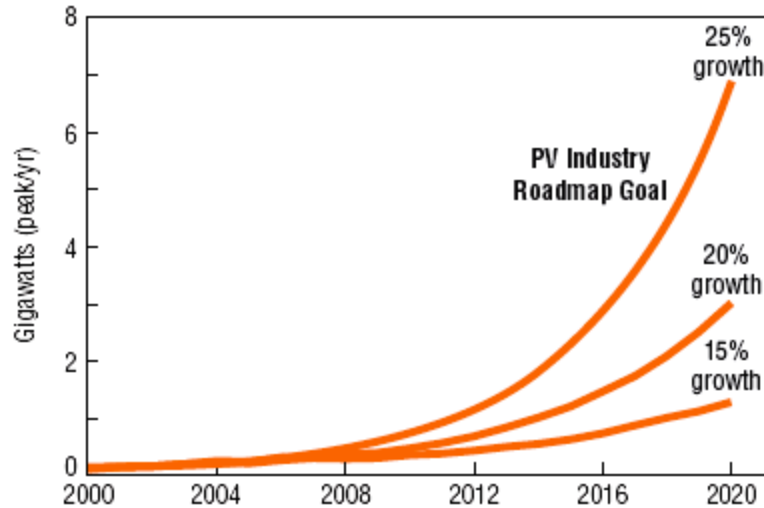


Figure 2. PV Roadmap Goal

of sunlight into electricity. The cost of PV has dropped down 15-20 fold and price reductions have helped to spur a growing market for photovoltaics. Shipments of PV modules have risen steadily over a past few years. With the manufacturing costs reducing steadily the average annual sales growth has also increased. To expand the markets, and to achieve the PV growth as shown in figure 2, PV costs need to be reduced further which can be achieved through research and development and technology transfer, a path that both industry and federal government are pursuing [3].

1.3 Beyond Single Crystal Silicon

Silicon is not only the material that will respond to sunlight by generating electron hole pairs, many semiconductors have similar properties. The silicon band gap of 1.1eV is workable but not ideal. One of the scientific discoveries of the semiconductor industry that has shown great potential for PV industry is thin film technology. Thin films can be made from variety of materials and today's most important thin film materials are amorphous silicon (α -Si), cadmium telluride (CdTe) and copper indium diselenide (CIS). The best laboratory efficiencies for these three thin films is shown in figure 3 [4].

Amorphous silicon is a growing segment in solar market as it can be manufactured at a lower cost than crystalline silicon. Researchers at National Renewable Energy Laboratory demonstrated fabrication of CIS with added gallium devices with efficiencies upto 19% [4]. Industry is exploring a new processing system for large area CIGS deposition. Using the new system, Institute of Energy Conversion (IEC) produced Solar cell that reached 14.9% efficiency. This system was designed to use on inline process and work is going on to manufacture CIGS based solar electric modules [4].

Cadmium Telluride has several features that make it a promising material for solar electric generation. These include the bandgap, which is well matched to solar spectrum and a high absorption coefficient, meaning even one micron thickness is sufficient to produce solar cell efficiency of 10% or higher. To date 10 techniques have been developed to fabricate CdTe solar cells with efficiencies upto 15%-16% [4]. Three of these methods are currently used for module fabrication by industry and module efficiencies of 10-11% have been achieved [4].

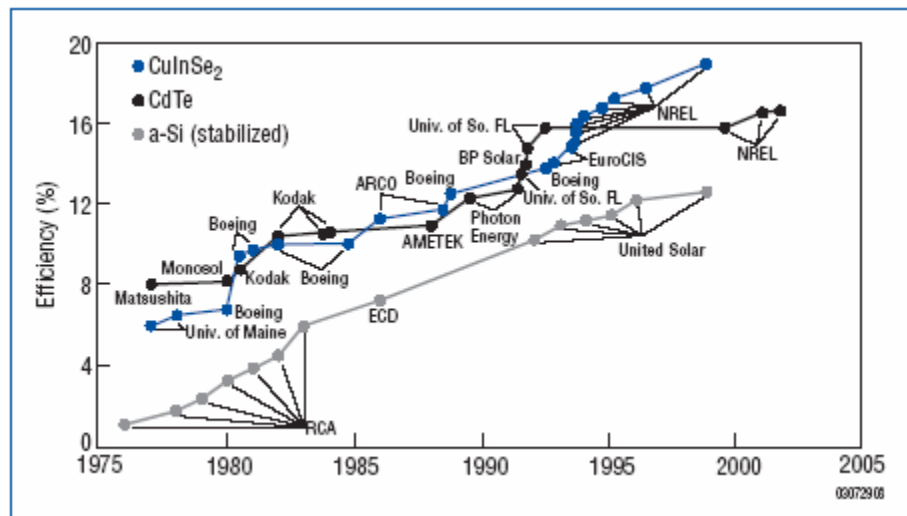


Figure 3. Best Laboratory Cell Efficiencies for Thin Films

In order to achieve higher efficiencies greater than 25% we need to develop tandem structures with top cell efficiencies up to 16-18%. $\text{Cd}_{1-x}\text{Zn}_x\text{Te}$ with a tunable bandgap of 1.45-2.2eV is suitable as a top cell with the bottom cell having a bandgap of 1eV. The main objective of this thesis is to study and fabricate high band gap $\text{Cd}_{1-x}\text{Zn}_x\text{Te}$ solar cells on glass and polyimide substrates by sputtering that could well serve in next generation solar cell technologies.

CHAPTER 2

THEORY OF SOLAR CELLS

2.1 Solar Power

The energy of the sun, according to current knowledge, is created by the nuclear fusion reaction of hydrogen to helium. This reaction takes place inside the star at several million degrees. The mass reduction occurring in this process is converted to energy. Since all elements are ionized to some degree at this temperature and their spectral lines are strongly broadened, the radiation consists of a multitude of spectral lines, so that the gaseous surface of the sun radiates like a black-body at 6000 K. In space solar radiation is obviously unaffected by earth's atmosphere and has power density of approximately 1365 W/m^2 . The characteristic spectral power distribution of solar radiation

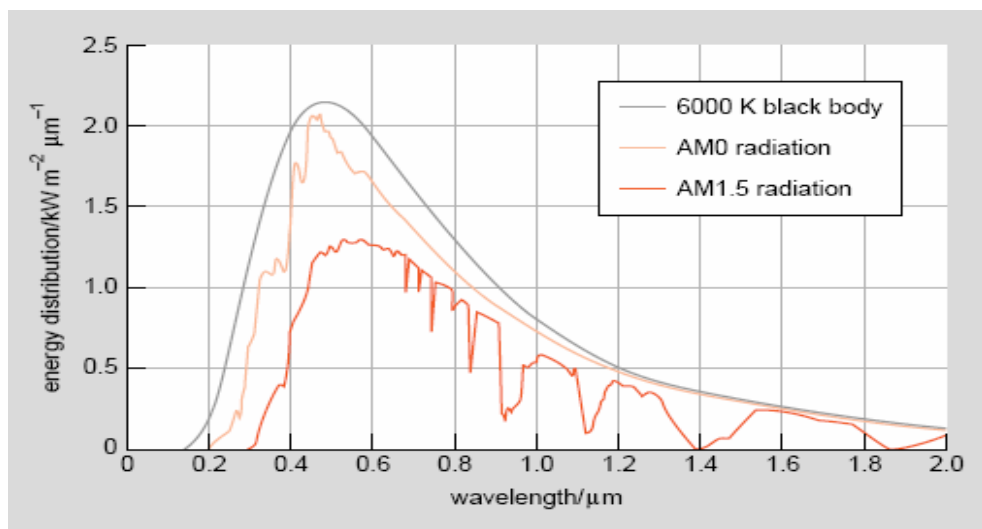


Figure 4. Solar Spectrum

as measured in space is described as Air Mass Zero (AM 0) distribution. At the earth's surface solar radiation is attenuated selectively at different wavelengths because of absorption by the atmosphere's constituent gases (oxygen, ozone, water vapor, carbon dioxide, etc). Because of constantly changing position of the sun, the light path through the atmosphere also changes. The spectral power distribution observed when sun's radiation is coming from an angle to overhead of about 48° corresponds to Air Mass 1.5 distribution which is the standard used for terrestrial applications and its total power density is 844 W/m^2 [5].

2.2 Solar Cell Parameters

Photovoltaic energy conversion requires the separation of electrons and holes by an internal electric field. When light made up of photons with energy larger than the bandgap is incident on the junction, it will be absorbed by the semiconductor and electron-hole pairs are created. These electron hole pairs are separated by an internal electric field and this gives rise to photocurrent. These charges lower the built-in potential of the junction, V_{bi} to $V_{bi} - V_{oc}$ where V_{oc} is open circuit voltage [5]. The generation rate of EHP in the bulk region is determined by the illumination flux and optical absorption constant of the semiconductor. The current voltage (I-V) characteristics of an ideal diode under dark are given by,

$$I = I_0 \{ \exp^{qV/KT} - 1 \}$$

Where I is the external current flow, I_0 is the reverse saturation current, q is the fundamental electronic charge of 1.602×10^{-19} Coulomb, V is the applied voltage, K is the Boltzmann constant and T is the absolute temperature.

A non-ideal solar cell can be described with an equivalent-circuit model. The most simple equivalent circuit used consists of a non-ideal diode, representing the p-n junction, coupled with a current source to account for the collection of light-generated carriers. A shunt resistance R_{sh} and a series resistance R_s are also included in the circuit. The complete equivalent-circuit diagram is shown in figure 5.

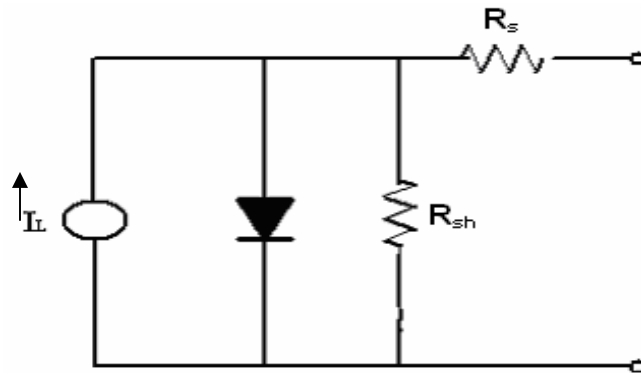


Figure 5. Equivalent Circuit of a Solar Cell

The series resistance R_s is the resistance the carriers find on their way and there are many effects that give rise to this resistance:

- Low conductivity of the window layer or of the absorber.
- Non-ohmic contacts.
- Recombination of carriers.

The shunt resistance is included to model is due to the effect of low resistivity of some parts of the material, such as grain boundaries or secondary phases and the effect of pinholes. The series resistance can be minimized by reducing the contact resistance and the shunt resistance can be maximized by reducing shunt paths in the junction [6].

Under AM 1.5 illumination the I-V characteristics are simply shifted down due to light generated current I_L as shown in figure 6,

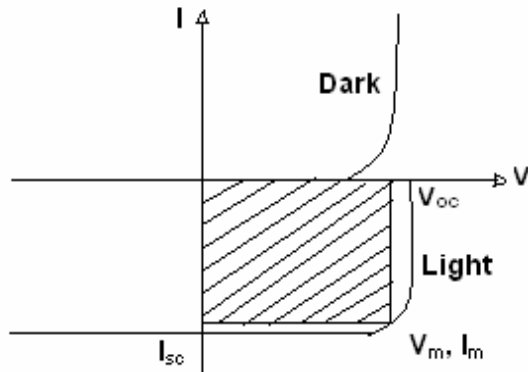


Figure 6. Dark and Light I-V Characteristics of a Solar Cell

Under illumination the theoretical behaviour is represented by,

$$I = I_0 \{ \exp^{qV/KT} - 1 \} - I_L$$

The curve describes three important parameters that give complete description of solar cell, open circuit voltage (V_{oc}), short circuit current (I_{sc}) and fill factor (FF).

under open circuit conditions, no current flows through the device and V_{oc} is observed at terminals of the junction. This quantity is unaffected by series resistance losses in the cell but is sensitive to shunt losses. Under short circuit conditions the entire light generated current, I_{sc} is seen with near zero voltage. This value is primarily affected by series resistance losses in device. The Parameters described above represent the maximum values that it is possible to measure and their product is ideal power.

The fill factor is then defined as the the area of maximum power rectangle to the product of short circuit current and open circuit voltage,

$$FF = \frac{I_m * V_m}{V_{oc} * I_{sc}}$$

Where I_m and V_m are the current and voltage for maximum power output. The most important parameter of solar cell is photovoltaic conversion efficiency defined as ratio of output power to input power calculated as,

$$\eta = \frac{FF * V_{oc} * I_{sc}}{P_{in}}$$

Where P_{in} is the incident light power.

CHAPTER 3

LITERATURE REVIEW

3.1 Why Tandem?

The Bandgap of 1.45eV of CdTe films is nearly optimum for a single junction high efficiency solar cell. Polycrystalline thin film heterojunction solar cells fabricated from CdTe films have achieved efficiencies upto 16% [7]. However we need efficiencies >25%, so that the module efficiencies of 15% or higher can be achieved by which low cost electricity can be provided. This can be realized with a tandem structure which has a bandgap of 1.7eV and 1.0 eV for the upper and lower cells respectively.

Tandem structures can be two terminal or four terminal. The disadvantage of two terminal tandem structure is current matching between series connected top and bottom cell. The bandgaps are dictated by the requirement that the photocurrents from each cell must be matched to achieve maximum efficiency. If not, the cascade current will be limited by the cell generating the lowest current, and the efficiency will fall [8]. Temperature variations also play a important role in limiting the efficiency and the choice of optimum energy gap combination of four terminal or two terminal structures [9]. An alternative better design compared to two terminal tandem structure is a multijunction device with independent terminals for each cell. For this structure the ranges of acceptable bandgaps that produce the higher efficiency are considerably broader. The contour map of conversion efficiency of a-Si/c-Si four terminal tandem solar cell is

shown in figure 7 [10]. As shown in figure, the maximum efficiency exceeding 30% appears for a bandgap combination of 2.1/1.5 eV and 2.3/1.4eV. For a bandgap combination of 1.75/1.2ev, which corresponds to a-Si/c-Si tandem device, more than 28% efficiency can be seen.

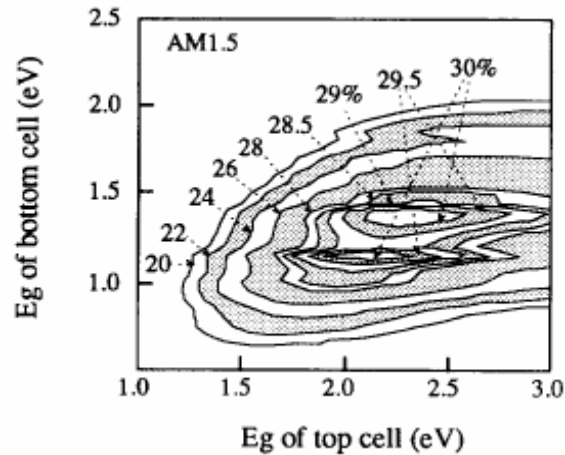


Figure 7. Contour Map of Conversion Efficiency of a Tandem Device

$Cd_{1-x}Zn_xTe$ is the one choice for the top cell in four terminal tandem structures as its bandgap can be varied between 1.45-2.2eV by varying the Composition value. While the ternaries are complex they offer flexibility of tuning the bandgap to bottom cell.. Using Penn State EPRI AMPS code for tandem simulations an efficiency more than 25% was predicted for $Cd_{1-x}Zn_xTe/CIGS$ tandem structure [11]. A four terminal tandem structure with with CIGS as bottom cell and $Cd_{1-x}Zn_xTe$ as top cell is shown in the figure 8.

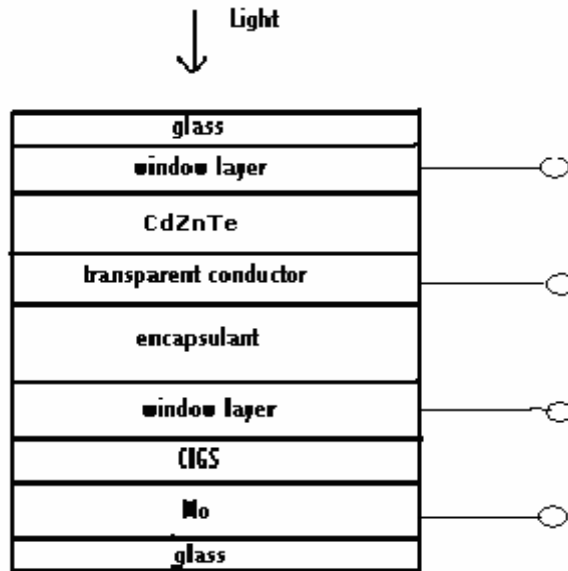


Figure 8. Four Terminal Tandem Solar Cell Structure

3.2 MBE Grown $\text{Cd}_{1-x}\text{Zn}_x\text{Te}$ Solar Cells

The ternary films of $\text{Cd}_{1-x}\text{Zn}_x\text{Te}$ were grown by MBE (Molecular beam epitaxy) on Glass/ SnO_2 / CdS Substrates with a target bandgap of 1.7-1.8eV. n-i-p $\text{Cd}_{1-x}\text{Zn}_x\text{Te}$ solar cells had better efficiencies compared to n-p cells. The optimum temperature was maintained at less than 400 °C. The substrates were baked out 250 °C for 3-4 hours with growth rate of 1 $\mu\text{m/hr}$. Before film growth the substrate temperature was kept at 275°C for 30minutes to commence film growth and increased to 300 °C for remaining run. Bandgap, compositional uniformity were determined by XRD technique. From the x-ray plot shown in figure 9, it is clear that there are no other mixed phase present in the $\text{Cd}_{1-x}\text{Zn}_x\text{Te}$ films since only peaks corresponding to $\text{Cd}_{1-x}\text{Zn}_x\text{Te}$ are observed. The lattice constant of $\text{Cd}_{1-x}\text{Zn}_x\text{Te}$ film was determined by extrapolation method used to estimate zinc content in films according to $a(x)=6.481-0.381x \text{ \AA}$ [7]. The zinc concentration was 0.4 corresponding to a bandgap of 1.7eV.

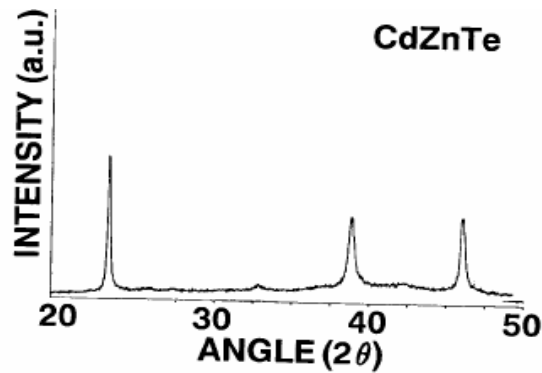


Figure 9. XRD of MBE Grown CZT

Both n-p and n-i-p $\text{Cd}_{1-x}\text{Zn}_x\text{Te}$ devices were fabricated, for n-i-p p-type ZnTe was deposited before contact metallization. The n-i-p spectral response was higher over most of the spectral range as shown in figure 11.

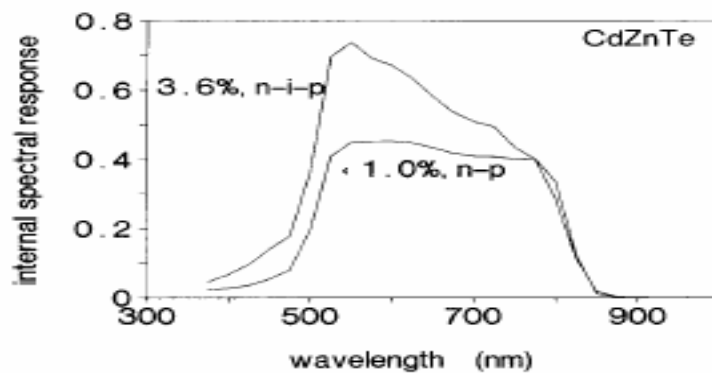


Figure 10. Spectral Response of n-p and n-i-p CZT Solar Cells

From spectral response we can see that bandgap was reduced from 1.7eV to 1.55eV after processing. This bandgap shift can be attributed to loss of zinc from its substitutional sites in the film. Auger depth profile analysis on this film after processing indicated a non uniform distribution of Te throughout the film with some zinc segregation to the ZnTe/ $\text{Cd}_{1-x}\text{Zn}_x\text{Te}$ interface within the bulk film. This possibly indicates that Zn has

left its lattice sites in $Cd_{1-x}Zn_xTe$ and may be forming other defect complexes which result in lowering of bandgap.

3.3 Effect of Pre-contact Treatments on $Cd_{1-x}Zn_xTe$ Films

Effect of $CdCl_2$ and $ZnCl_2$ treatment were observed in single phase $Cd_{1-x}Zn_xTe$ alloy films deposited by a co-evaporation from binary $CdTe$ and $ZnTe$ sources of thickness 3-4 μm with bandgap varying between 1.5-2.25eV [12]. Efforts to directly implement $CdCl_2$ treatment on $Cd_{1-x}Zn_xTe$ films similar to $CdTe$ films did not work out due to high reactivity of $ZnTe$ with $CdCl_2$. $Cd_{1-x}Zn_xTe$ was fabricated on 7059/ITO/ CdS substrates and XRD was used to determine phase changes and alloy distribution in the films after treatments in argon, dry air, $CdCl_2$ vapor + dry air and $ZnCl_2$ vapor +dry air which are summarized below.

Table 1. Conditions and Results of 15minute Pre-Contact Treatments on CZT

Film Temp (°C)	Ambient	XRD orientation	Phases
600	Argon	(220)	$Cd_{0.6}Zn_{0.4}Te$
450	Dry air	(111)	$Cd_{0.6}Zn_{0.4}Te \rightarrow CdTe, ZnO, Te, TeO_2$
420	2mTorr $ZnCl_2:O_2:Ar$	(111)	$Cd_{0.6}Zn_{0.4}Te, ZnO$ trace, Te trace
420	9mTorr $ZnCl_2:O_2:Ar$	(111)	$Cd_{0.6}Zn_{0.4}Te, ZnO,$ Te trace
420	1Torr $ZnCl_2:O_2:Ar$	(random)	$Cd_{0.6}Zn_{0.4}Te \rightarrow$ $Cd_{0.6}Zn_{0.2}Te,$ $Zn(ClO_4)_2, Te$
420	2mTorr $CdCl_2:O_2:Ar$	(111)	$Cd_{0.6}Zn_{0.4}Te \rightarrow CdTe,$ ZnO, Te
420	9mTorr $CdCl_2:O_2:Ar$	(111)	$CdTe \rightarrow Cd_{0.6}Zn_{0.4}Te,$ ZnO trace

From above results table we can infer that ,

- Treatment in argon at 600 °C only causes primary recrystallization.
- Treatment in dry air preferentially removes ZnTe from the alloy as oxides.
- Treatment in ZnCl₂:O₂:Ar at low pressure, preserves the bulk alloy composition.
- Treatment in ZnCl₂:O₂:Ar at high pressure, removes ZnTe from alloy as ZnO and Te.
- Treatment in CdCl₂:O₂:Ar removes ZnTe from the alloy forming CdTe ,ZnO, Te and volatile ZnCl₂.

Devices were fabricated similar to CdTe/CdS but utilizing selected post deposition treatments. Back contact was formed by sequential deposition of Te and Cu layers by electron beam evaporation, application of graphite ink and heat treatment at 100 °C for 30min. However these devices exhibited significant dark-light crossover and low J_{sc}. These properties suggest poor conductivity and poor carrier transport in the absorber layer. Spectral response measurements of ZnCl₂ treated devices show low collection and long wavelength fall off at 720nm corresponding to as-deposited bandgap of 1.7eV.

3.4 Contact Technology

The formation of a stable, reproducible, low resistance contact to p- Cd_{1-x}Zn_xTe is one of the major problems in fabrication of efficient solar cells. The reason for this is high work function of Cadmium zinc Telluride. CZT with a bandgap of 1.7eV has a work function of ~5.2eV [13] . No metals present such a high value and thus most of the contacts are rectifying. Metals like platinum satisfy the condition for ohmic contacts on p-type CZT, however the stability of the contact for solar cell purposes is questionable. Electrical properties of contacts on p-type Cd_{0.8}Zn_{0.2}Te were studied. Au, Al, In and electroless Au

were used for this purpose. Results showed that electroless Au films deposited by chemical method can form a heavily doped p+ layer on Cd_{0.8}Zn_{0.2}Te smooth surface which is nearly ohmic on p-type material. The CZT films were pre-contact treated with bromine methanol (BM etchant) followed by lactic in ethylene glycol (LB etchant). Post annealing treatments were also found to improve ohmic quality and adhesion of contact layers to Cd_{0.8}Zn_{0.2}Te surface [14]. ZnTe:Cu contact is one of the contact that has been successfully used in CdTe/CdS solar cells [15]. Research has shown that reproducible p-type doping of ZnTe can be achieved by reactive RF magnetron sputtering with Ar/N₂ gas mixtures eliminating the need for Cu doping [16]. In our case ZnTe was deposited in RF magnetron sputtering chamber with Ar/N₂ gas mixture and doped graphite was used as metal contact.

3.5 Thin Films on Flexible Polyimide Substrates

In recent years there has been an increased interest in photovoltaic structures on light weight flexible substrates. Photovoltaic structures on lightweight substrates have several advantages over the heavy glass based structures in both terrestrial and space applications [17]. They are important for novel added products such as portable and lightweight sources of power for emergencies and recreational use, PV integrated buildings, Solar boats and cars, smart cards, data and telecommunication products [18]. CdTe Solar cells with a efficiency of 8.6% [18] and CIGS solar cells with efficiency of 11.3% [20] were fabricated on polyimide substrates for both terrestrial and space applications. A lot of work has been done on TCO's such as ITO and ZnO:Al deposited on polyimide which have good optoelectronic properties [19]. Reported difficulties while processing with polyimide substrates include low processing temperatures and poor adhesion of films.

ITO films were deposited on Kapton polyimide by RF sputtering at room temperature. Before the deposition process plasma etching on the surface of the substrates was done with low N_2 flows and low power of $1W/cm^2$ to improve adhesion of ITO on polyimide [19]. The thickness on the glass reference sample was around 500nm. From the XRD data as shown in figure 11, we can see that ITO polycrystalline films are grown with preferred (222) orientation. The average transmission of ITO on polyimide was found to be 72.5% as seen in figure 11 with sheet resistance of about $14 \Omega / \square$.

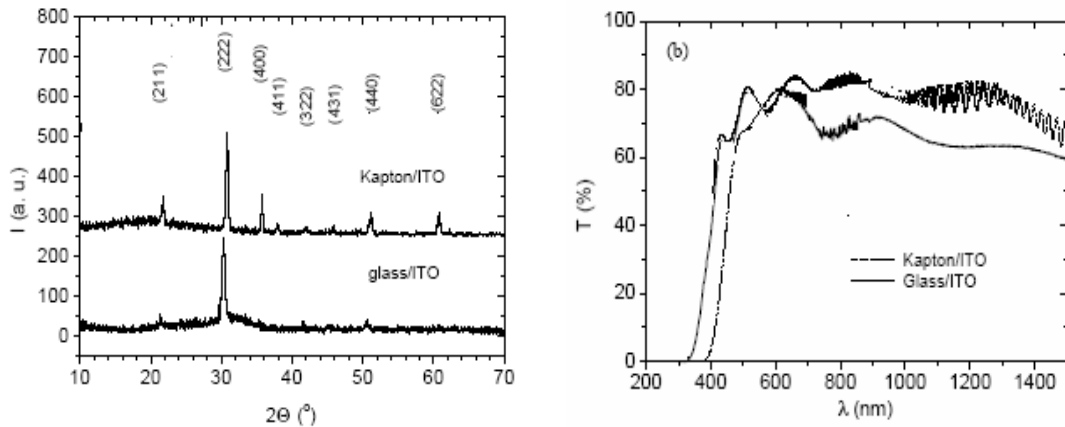


Figure 11. XRD(Left) and Transmission(Right) of ITO on Polyimide and Glass

CdTe solar cells were fabricated on polyimide substrates, but instead of commercially available polyimide, a specific type of polyimide was prepared in house [18]. One of the advantages of this is that the thickness of polyimide film can be minimized thereby reducing the absorption loss in the substrate. A thin buffer layer was evaporated onto the glass substrate, then a polyimide layer was spin coated and cured at $430^{\circ}C$. CdTe/CdS solar cells were fabricated on this spin coated polyimide substrate with a process in which all layers were grown by evaporation method. After complete processing the entire stack was separated from glass by dissolving NaCl buffer layer in water. The structural

properties of CdTe on polyimide were similar to that of glass substrates. As shown in figure 12 as deposited CdTe layer is compact with grain size upto $\sim 1\mu\text{m}$.



Figure 12. SEM of As deposited (Left) and CdCl₂ Treated (Right) CdTe/CdS/O/Poly

The CdCl₂ treated layers are crack free with grain size upto $\sim 5\mu\text{m}$. The as deposited layers had (111) orientation, but loss in orientation was observed in CdCl₂ annealed samples [21]. The I-V Characteristics of CdS/CdTe solar cell on polyimide is shown in figure 13. Efficiencies upto 8% were obtained on polyimide substrate. The lower efficiencies are attributed to high resistivity of TCO ZnO:Al films which do not yield efficient CdTe/CdS solar cells. Higher efficiencies can be expected if the same process is done on ITO or SnO₂ front contacts[18].

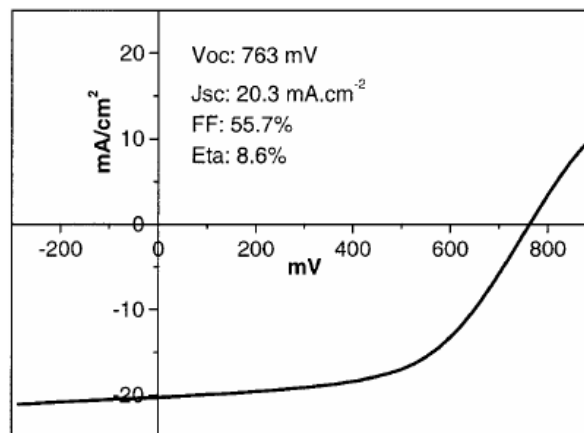


Figure 13. I-V Characteristics of CdTe Solar Cell on Polyimide

CHAPTER 4

PROCESSING

4.1 Cell Structure

High performance multijunction tandem solar cells based on polycrystalline thin films will require a wide band gap top cell with atleast 15% efficiency. This work aims to study the feasibility of $\text{Cd}_{1-x}\text{Zn}_x\text{Te}$ solar cell as the top cell with a band gap of 1.7eV on glass and polyimide substrates. The basic cell structure of CZT solar cell on glass and polyimide substrate is shown in figure 14. The processing of each layer is described in the later part of the chapter.

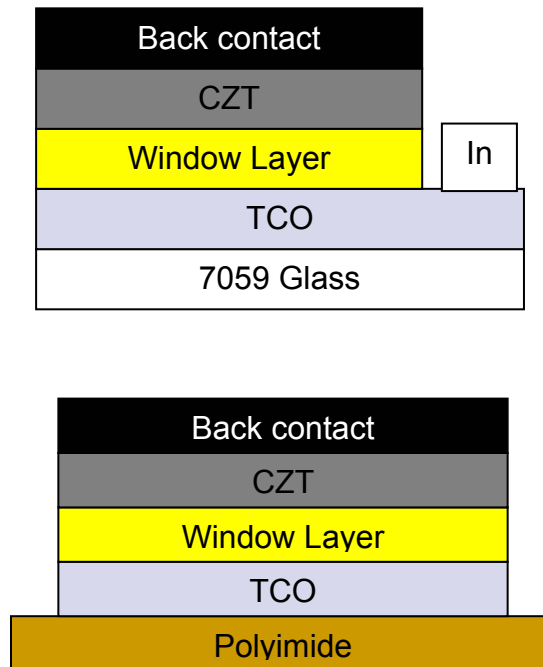


Figure 14. CZT Solar Cell Structure on Glass (top) and Flexible Polyimide Substrate (bottom)

4.2 Deposition Technique

4.2.1 Transparent Conducting Oxides

Transparent conducting oxide (TCO) acts as a Front Contact for a solar cell. Ideally for a solar cell the TCO should have low resistivity and optical transmission greater than 90% [22]. Tin Oxide(SnO_2) or Indium Tin Oxide (ITO) were used as transparent conducting oxides for our experiments. SnO_2 was deposited by MOCVD technique with O_2 and Tetramethyltin (Tin source). High purity helium is used as a carrier gas. The thickness of this film is $\sim 700\text{-}800 \text{ \AA}$. Indium tin oxide(ITO) is deposited by a 3" RF magnetron sputtering with Ar as plasma source. The total pressure was maintained at $2\text{-}3 \times 10^{-3}$ torr at $200\text{-}300 \text{ }^\circ\text{C}$ substrate temperature. The thickness of these films is about $1500\text{-}2000 \text{ \AA}$. Both the films had resistivity less than $2 \times 10^{-4} \text{ } \Omega\text{-cm}$ and transmission greater than 90%.

4.2.2 Window Layer

Cadmium sulphide (CdS) or Zinc selenide (ZnSe) were used as a window layers to form the junction with p-type absorber layer. CdS has a proven record of highest efficiencies with CdTe solar cells. CdS in this case was deposited by chemical bath deposition with a cadmium salt ,ammonium salt, ammonia and thiourea as the reactants used in aqueous solution. The amount of ammonia and ammonium salt can be used to control CdS deposition rate [23]. The solution was heated to $80\text{-}85 \text{ }^\circ\text{C}$ during the process and final thickness obtained is $< 1200 \text{ \AA}$. ZnSe is deposited in a 3" RF magnetron sputtering chamber with Ar as plasma source. The substrate is heated upto $250\text{-}300 \text{ }^\circ\text{C}$ and pressure is kept at $4\text{-}5 \times 10^{-3}$ torr. The thickness is varied between $500\text{-}1000 \text{ \AA}$ in different cases.

4.2.3 Cadmium Zinc Telluride

Cadmium Zinc Telluride (CZT) is the absorber layer. CZT was deposited in a RF magnetron co-sputtering chamber with 99.999% purity CdTe and ZnTe sources. For high efficiency tandem solar cell we need a top cell with a bandgap of 1.7eV. This can be achieved by varying the composition of CdTe and ZnTe, so that bandgap can be varied from 1.45eV-2.2eV. The set up for depositing CZT is shown in figure 15. A Varian CRYOSTACK-8 Cryo pump is used to evacuate the chamber to a base pressure in the range of 10^{-7} torr and sputtering pressure is maintained between $4-5 \times 10^{-3}$ torr with Ar/N₂ mixture as the plasma source. The thickness on the substrate was monitored using crystal monitor.

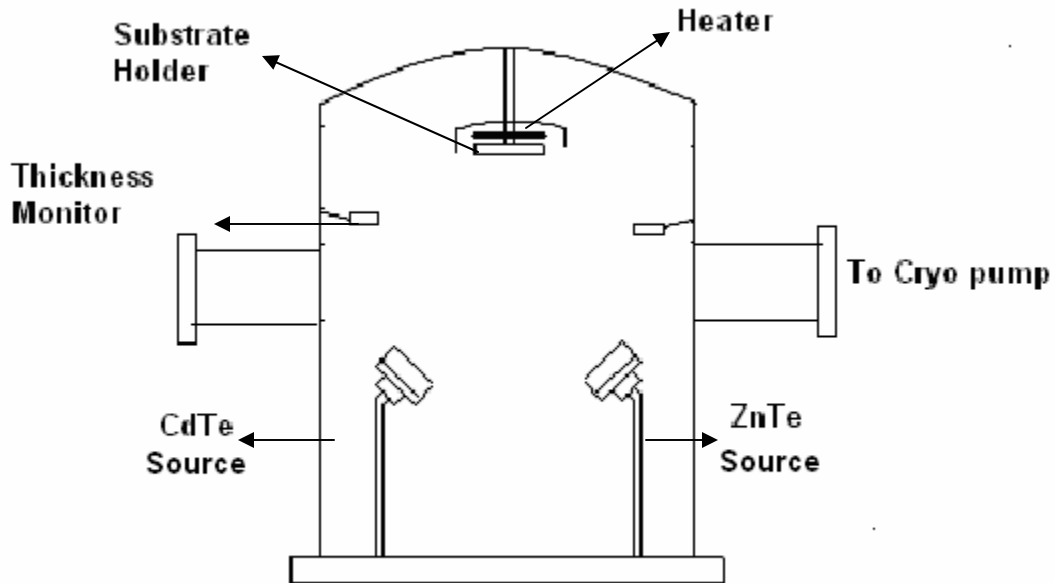


Figure 15. Co-sputtering Chamber for CZT Deposition

Thickness calibration and temperature calibration were done before starting actual experiments. A THERMCOAX heater is used as substrate heating element. The

calibrated temperatures for substrate are shown in table 2. Substrate holder is rotated during deposition to get uniform heating on the substrate and uniform deposition. The thickness of the films is maintained between 4-5 μm .

Table 2. Calibrated Substrate Temperatures

Heater Temperature ($^{\circ}\text{C}$)	Substrate temperature ($^{\circ}\text{C}$)
600	400
500	300
420	200

4.2.4 Back Contact

Graphite paste doped with HgTe:Cu is one of the contact used for CZT solar cells. ZnTe is the other back contact that was used. For our experiments ZnTe is deposited in RF magnetron sputtering chamber with Ar/N₂ gas mixture and doped graphite is used as metal contact.

4.3 Measurements

4.3.1 Spectral Response

The quantum efficiency is the measure of number of electron-hole pairs generated and collected for every incident photon absorbed. The external quantum efficiency of the device is determined and plotted as function of wavelength. A spectrometer is used which has a grating. By varying the angle of grating to incident light, monochromatic light of different wavelengths can be produced. The source is calibrated from silicon standard cell obtained from the National Renewable Energy Laboratory (NREL). The output J_{sc} , of

the cell at each wavelength is normalized against the same for the Si standard cell. The plot of external quantum efficiency versus wavelength is plotted.

4.3.2 I-V

All the devices were characterized by light and dark current-voltage(I-V) measurements and the main device parameters like V_{oc} , J_{sc} , FF and efficiency were determined. Light I-V measurements were taken with a computer controlled Keithley source meter. Light from four OSRAM halogen lamps simulated the AM 1.5 solar spectrum and provided uniform distribution over an area large enough to place a sample (4x4) cm. A labview program runs in the computer which is used to control sweep voltage across the device. Once the currents are logged the program calculates main device parameters and characteristic dark and light I-V curves are plotted.

4.3.3 SEM and XRD

The structural properties of CZT films were characterized by X-ray diffraction (XRD) and Scanning electron microscopy (SEM). XRD measurements were done using Philips X'pert PRO X-ray diffraction system and SEM micrographs were taken on a Hitachi 800 SEM system.

CHAPTER 5

RESULTS AND DISCUSSION

5.1 CZT Material Properties

5.1.1 Optical Properties

The CZT films optical properties were characterized by transmission measurements. As discussed in previous chapter CZT was deposited in a co-sputtering chamber with Ar/N₂ mixture as the plasma source. The deposition was carried out with a total pressure of $4-5 \times 10^{-3}$ torr and substrate temperature in the 300-400 °C range. Initial experiments were carried out to obtain a bandgap of 1.7eV. Transmission and bandgap

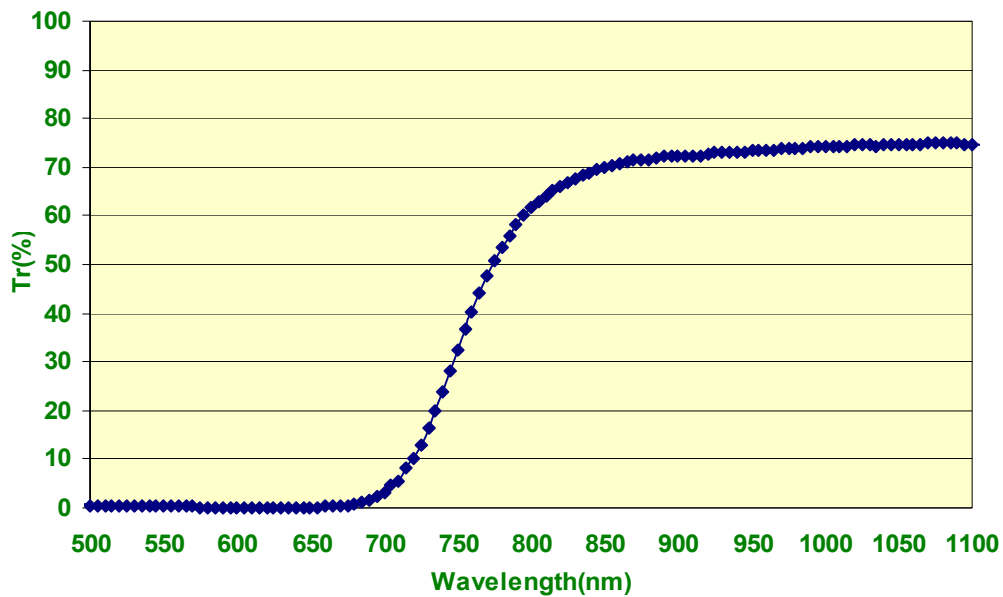


Figure 16. Optical Transmission of CZT

measurements were done for each substrate. The transmission of CZT on Glass/SnO₂ substrate was around 70% as shown in figure 16. The optical bandgap of a material can be found from transmission spectra if the film thickness is known. Since $\alpha = \alpha_0(E - E_g)^{1/2}$ where E_g is the bandgap, E is the energy of incident photons, α_0 is the constant and α is the absorption co-efficient [25]. Then a plot of α^2 Vs photon energy(E) should yield a line with an intercept equal to E_g which shown in figure 17. The bandgap deduced from the plot is 1.7eV which is the desired bandgap for our experiments.

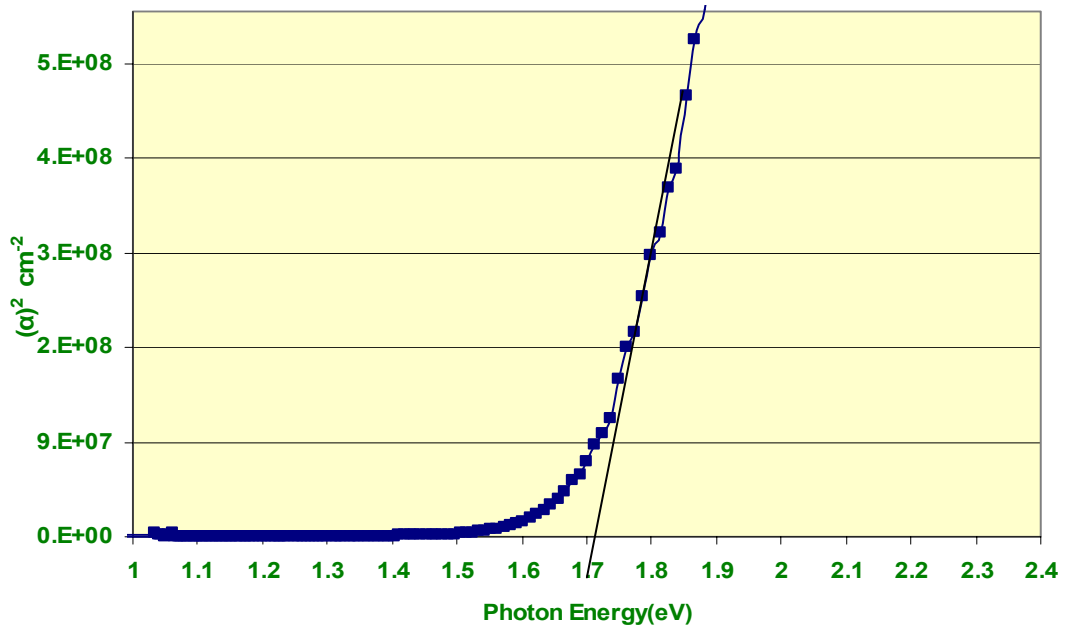


Figure 17. Measured Bandgap of CZT

5.1.2 Structural Properties

The structural properties of CZT films were characterized by using X-ray diffraction and scanning electron microscopy. For this purpose Glass/SnO₂/CZT substrates were used. CZT was deposited with Ar/N₂ mixture as plasma source at 400 °C and one set of samples were annealed in helium ambient so that measurements could be carried on

as-deposited and annealed samples. XRD measurements were done on the as-deposited and annealed SnO_2/CZT samples as shown in figure 18 to determine film

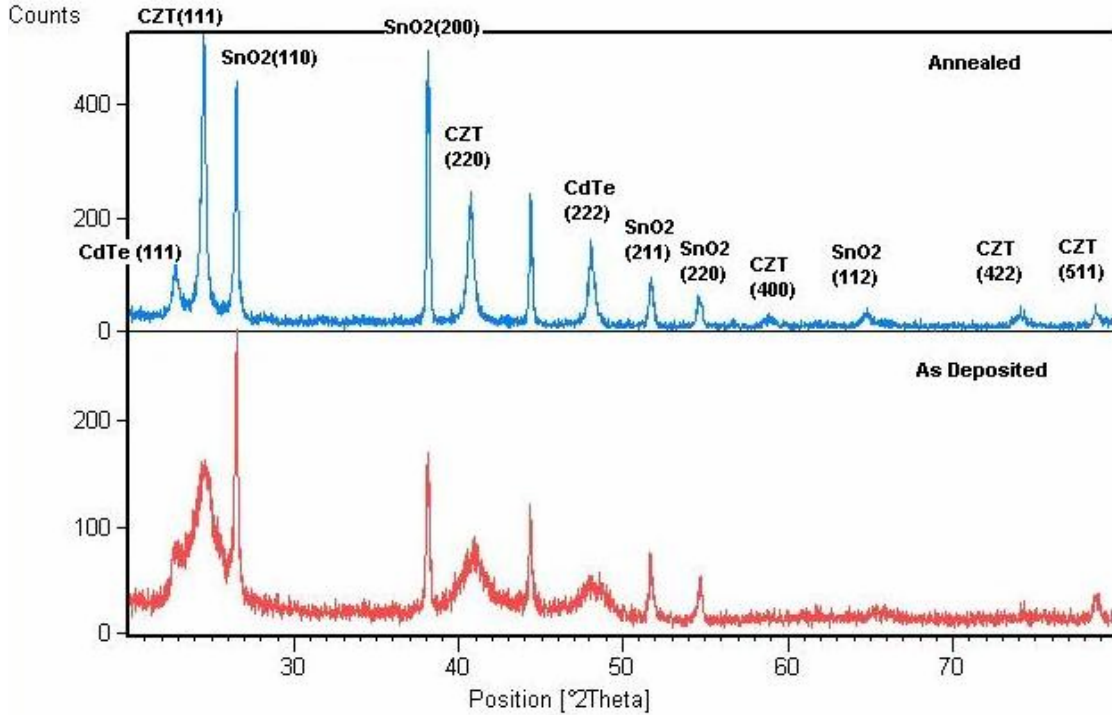


Figure 18. XRD of As Deposited and Annealed CZT Films

composition, orientation and possible formation of mixed phase. The as-deposited CZT films exhibit strong (111) texture. The zinc concentration in $\text{Cd}_{1-x}\text{Zn}_x\text{Te}$ was determined using the lattice constant relation $a(x)=6.481-0.381x \text{ \AA}$. The value of x is ~ 0.4 which is consistent with measured optical bandgap of 1.7eV. After annealing the intensity of (111) reflection increased and became sharper than as deposited films, all other reflections also sharpened with increased peak intensity which indicates annealing improved crystallinity of CZT films. It can be seen that both as-deposited and annealed films had CdTe peaks which gives hint of mixed phase.

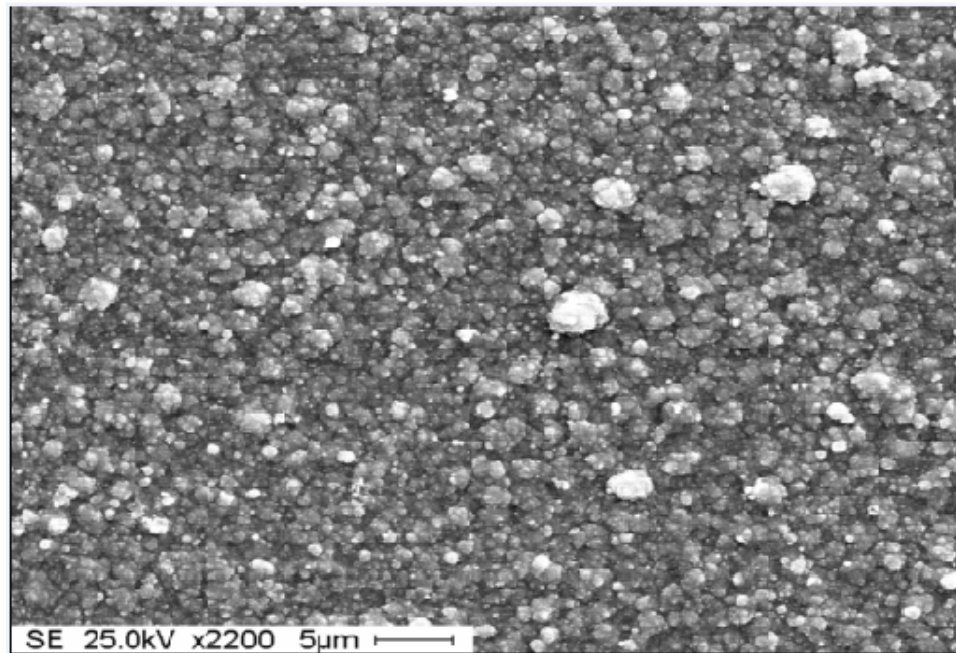
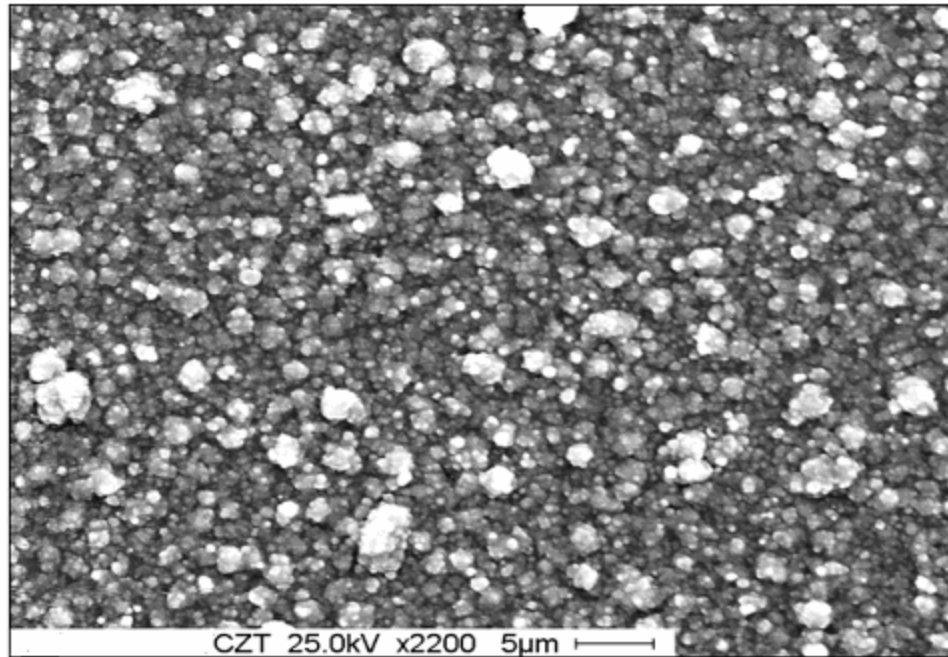


Figure 19. SEM of As Deposited(Top) and Annealed (Bottom) CZT Films on Glass/SnO₂ Substrate

SEM images for as deposited and annealed CZT films are shown in figure 19. From the results it can be seen that both as deposited and annealed films had closely packed dense structure with large number of small grains and SEM analysis did not reveal significant grain growth after anneal, which indicates anneal induced primary recrystallization without changing the alloy composition of the films.

5.2 CZT Solar Cells

5.2.1 Effect of N₂ on CZT Device Performance

Nitrogen doping of II-VI compounds has been successfully reported. High doping levels can be achieved with ZnTe and slightly lower for CdTe, but very low doping levels have been achieved with ternary compounds such as CdZnTe and CdMgTe, which might be due to formation of nitrides which act as a limiting factor [24]. After initial work on CZT films deposited with 50:50 Ar/N₂ mixture, our further work was concentrated on the varying N₂ partial pressure during CZT deposition and its effect on the CZT device performance. A series of experiments were conducted with varying N₂ partial pressure. These experiments were conducted on SnO₂/CdS and SnO₂ substrates. The total pressure was maintained at $4-5 \times 10^{-3}$ torr with Ar/N₂ mixture. The deposition was done at 300-400 °C and the N₂ partial pressure varied by 10%, 25%, 50%, and 75% of the total pressure. The devices were grouped into as-deposited and annealed. Annealing was carried out at 500 °C in Helium ambient and doped graphite was used as back contact for all these devices. The results are summarized below.

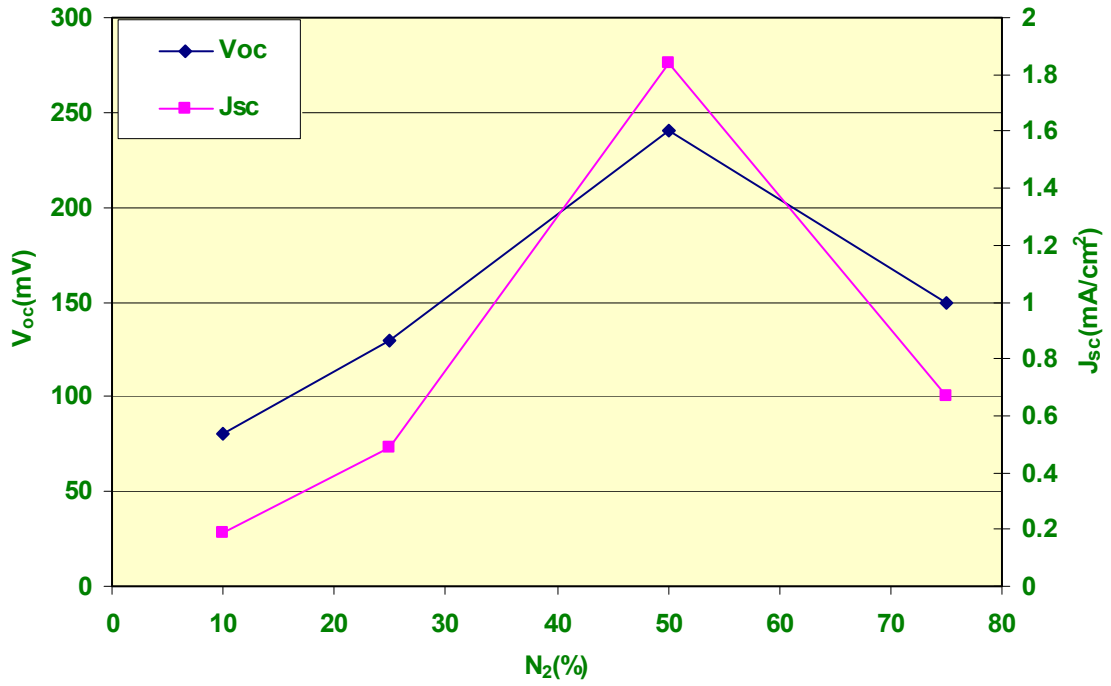


Figure 20. Effect of N₂ on V_{oc} and J_{sc} for As Deposited SnO₂/CZT Solar Cells

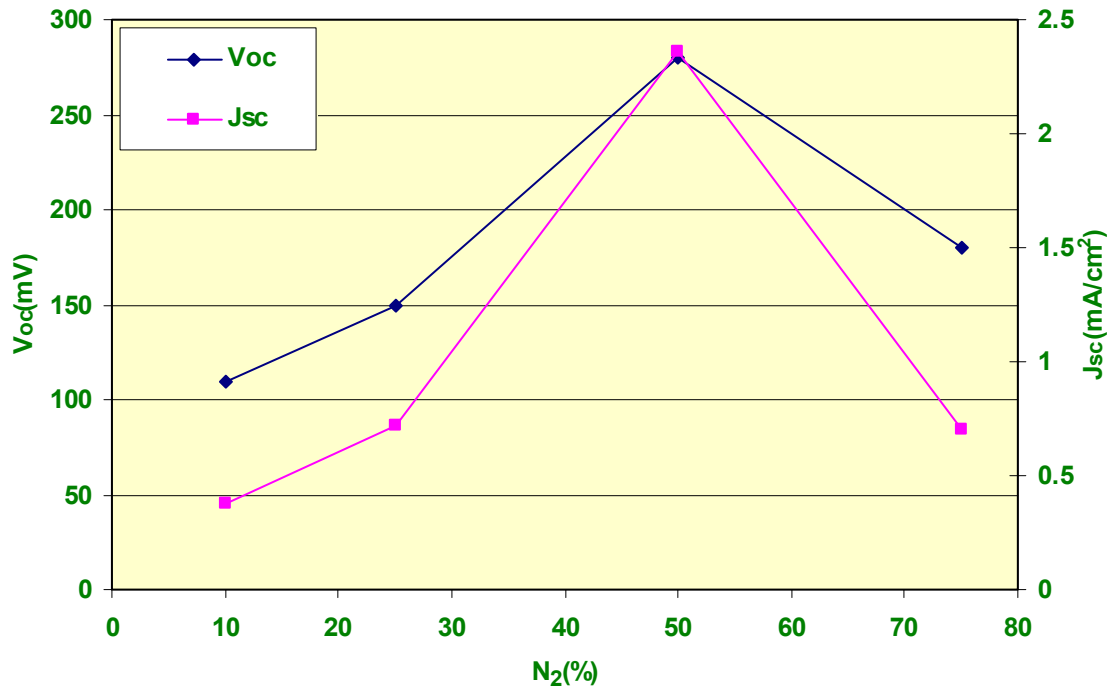


Figure 21. Effect of N₂ on V_{oc} and J_{sc} for Annealed SnO₂/CZT Solar Cells

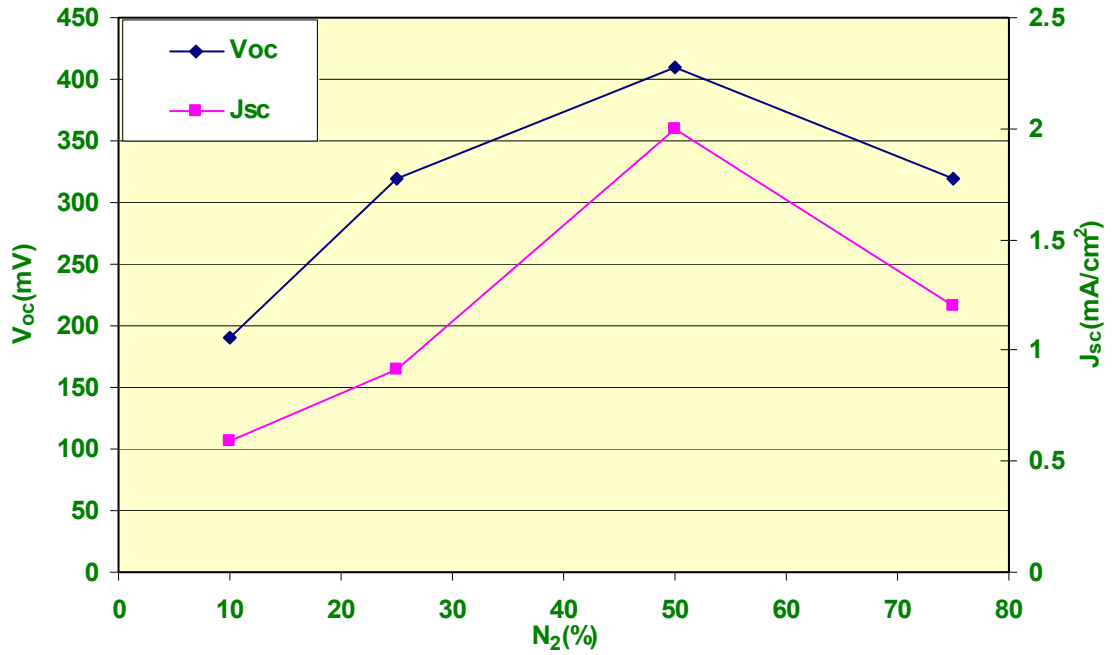


Figure 22. Effect of N₂ on V_{oc} and J_{sc} for As Deposited SnO₂/CdS/CZT Solar Cells

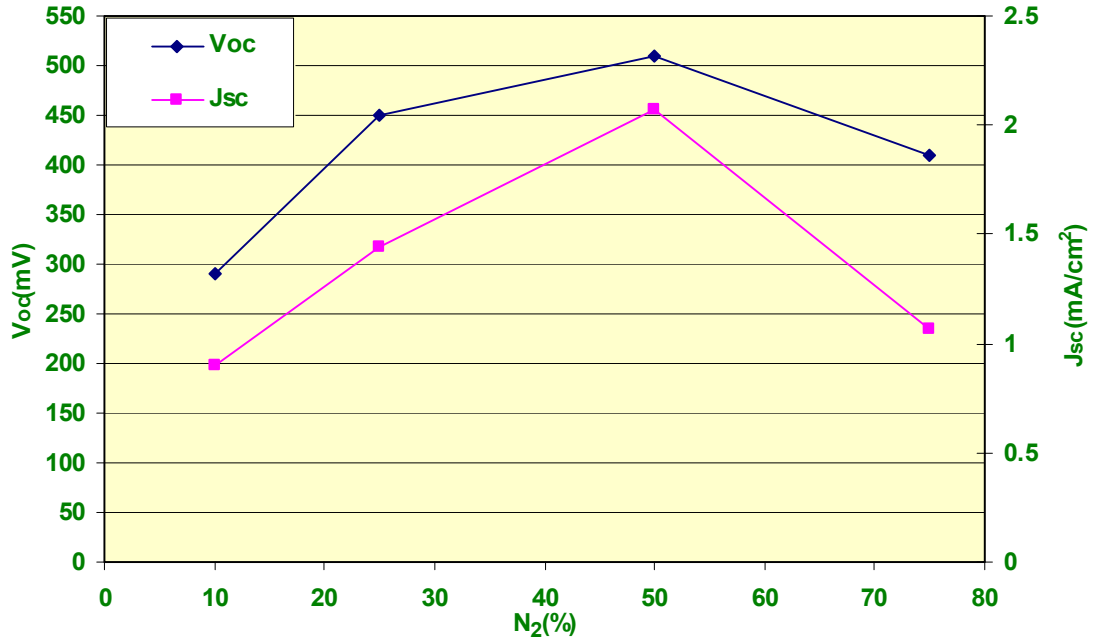


Figure 23. Effect of N₂ on V_{oc} and J_{sc} for Annealed SnO₂/CdS/CZT Solar Cells

From the above results it can be seen that N_2 concentration increases both V_{oc} and J_{sc} values in $SnO_2/CdS/CZT$ and SnO_2/CZT devices up to 50% N_2 partial pressure beyond which the CZT device performance degrades. This effect of N_2 is not exactly known but it can be speculated that N_2 improves electronic properties of CZT films even though the mechanism of which is not yet known. It can also be seen that annealing of CZT films helps to improve the performance of device irrespective of N_2 concentration.

5.2.2 ITO/ZnSe/CZT

After establishing deposition conditions for CZT with bandgap of 1.7eV, CZT solar cells were fabricated with ITO/ZnSe substrates. Both ITO and ZnSe were deposited by RF magnetron sputtering with Ar ambient at 200 -250 °C. The thickness of ITO was 1000-2000 Å and ZnSe was 500-1000 Å. CZT was deposited with Ar/ N_2 mixture as plasma source. The total pressure was $4-5 \times 10^{-3}$ torr with N_2 partial pressure of 2.5×10^{-3} torr. The processing was categorized into two groups, (a) as-deposited. (b) annealed. The samples were contacted with doped graphite. The films were annealed at different temperatures in Helium ambient to study their performance. The V_{oc} and J_{sc} values of as deposited and cells annealed in Helium at 450 °C and 500 °C are shown in figure 24. The fill factors of all the devices were less than 30%. Efforts to anneal at temperatures greater than 500 °C did not yield better results as the CZT films were evaporating.

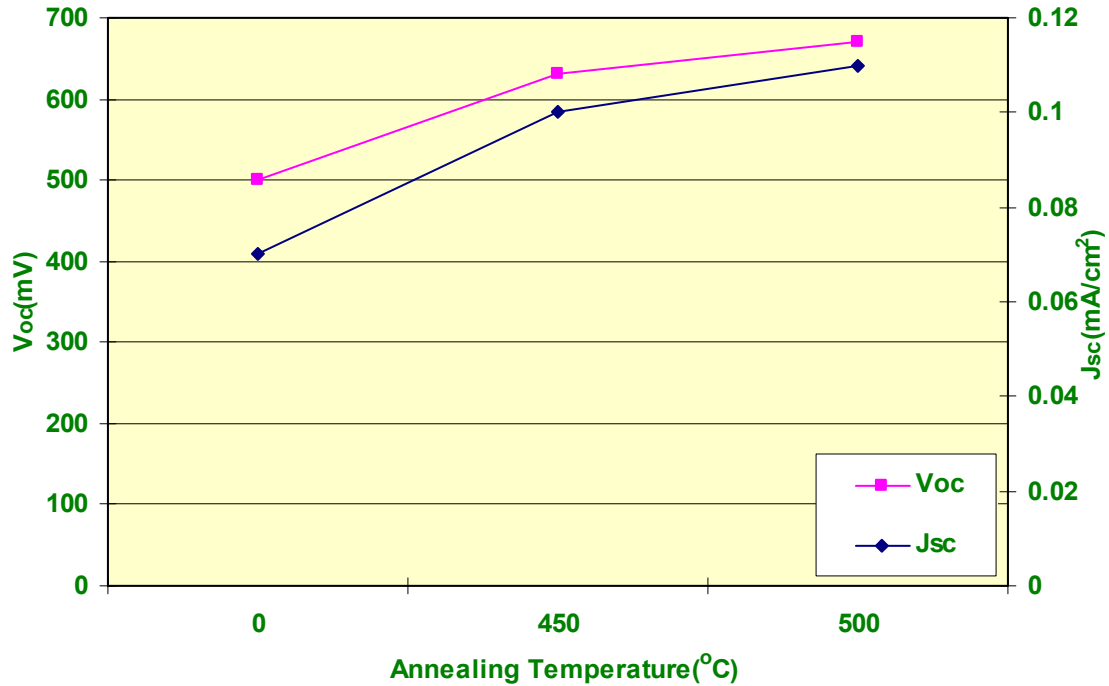


Figure 24. Effect of Annealing on ITO/ZnSe/CZT Solar Cells

The cells annealed at 500 °C exhibited better characteristics compared to other annealing temperatures. High V_{oc} 's were obtained for the films annealed at 500 °C but currents were less than 1mA/cm².

From the high V_{oc} values it can be speculated that annealing improves junction properties to some extent. The spectral response for the devices annealed at 500 °C is shown in figure 25, from which it can be seen that low collection in the 550-700nm region is the main cause for currents to be low . The J_{sc} of the devices calculated from the SR was less than 1mA/cm² which is well below the ideal value based on CZT bandgap which is around 22 mA/cm².

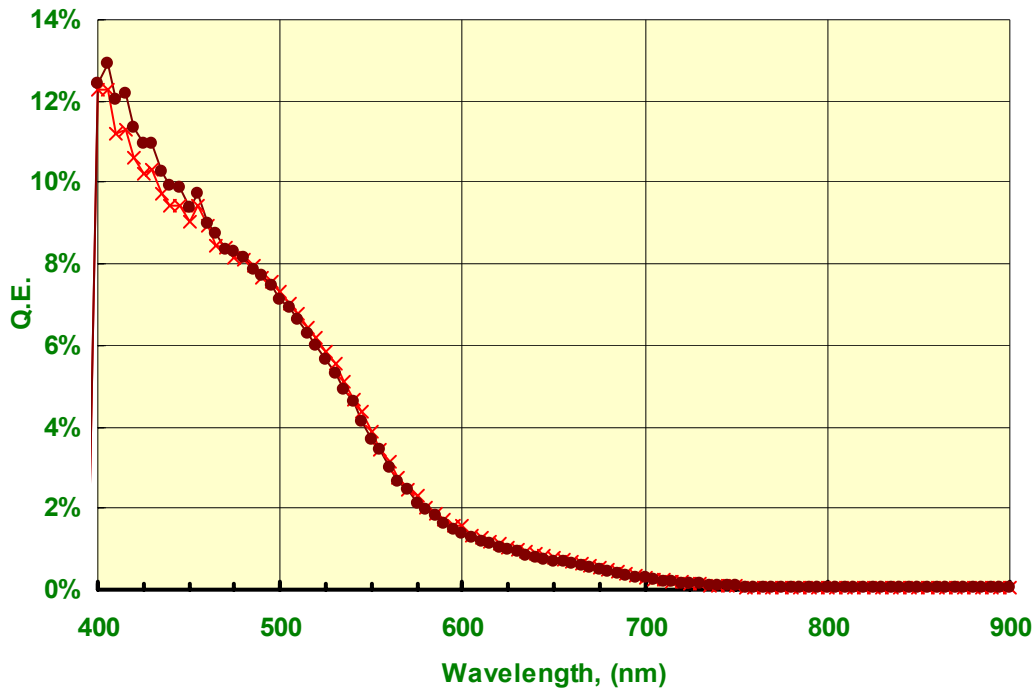


Figure 25. Spectral Response of Annealed ITO/ZnSe/CZT Devices

5.2.3 SnO₂/CZT and SnO₂/CdS/CZT

After studying ZnSe/CZT devices, CZT solar cells were fabricated with SnO₂ and SnO₂/CdS substrates. CZT was deposited with Ar/N₂ mixture as plasma source. The total pressure is $4-5 \times 10^{-3}$ torr with N₂ partial pressure of 2.5×10^{-3} torr. SnO₂ was deposited by MOCVD and CdS was deposited by chemical bath deposition. The devices were grouped into as-deposited and annealed. A temperature of 500 °C was chosen as annealing temperature for the devices as films above that temperature were evaporating. The samples were contacted with doped graphite. The results of as-deposited and samples annealed at 500 °C in He ambient are summarized in table 3.

Table 3. Comparison of As Deposited and Annealed CZT Devices on SnO₂ and SnO₂/CdS Substrates

Device structure	Pre contact condition	V _{oc} (mV)	J _{sc} (mA/cm ²)
SnO ₂ /CZT	As deposited	240	1.84
SnO ₂ /CZT	Annealed	280	2.36
SnO ₂ /CdS/CZT	As deposited	410	1.87
SnO ₂ /CdS/CZT	Annealed	510	2.07

From the results it can be seen that currents were comparable in SnO₂/CZT and SnO₂/CdS/CZT devices, however V_{oc}'s were high in SnO₂/CdS/CZT devices. It can also be seen that annealed devices had better V_{oc}'s and J_{sc}'s compared to as deposited devices in both the device structures. This shows that even though annealing did not increase the grain size of CZT films as shown in SEM micrographs in figure 19, it might have helped to improve some of the interface/junction properties and crystallinity of the films which resulted in high V_{oc}. The J-V and spectral response measurements were done on these devices and are summarized below. From the spectral response results it can be seen that low collection in 550nm-700nm region leads to low currents. The cause for this low collection is not exactly known but it may be due to carrier recombination within the bulk before they reach the junction and proceed to external circuit or may be due to low electric field in the space charge region. Therefore it can be speculated that sputtered CZT films have poor electronic properties. The fill factors of all the devices were less than 30%. From the J-V curves it can be seen that devices have high series resistance which contributes to low fill factors.

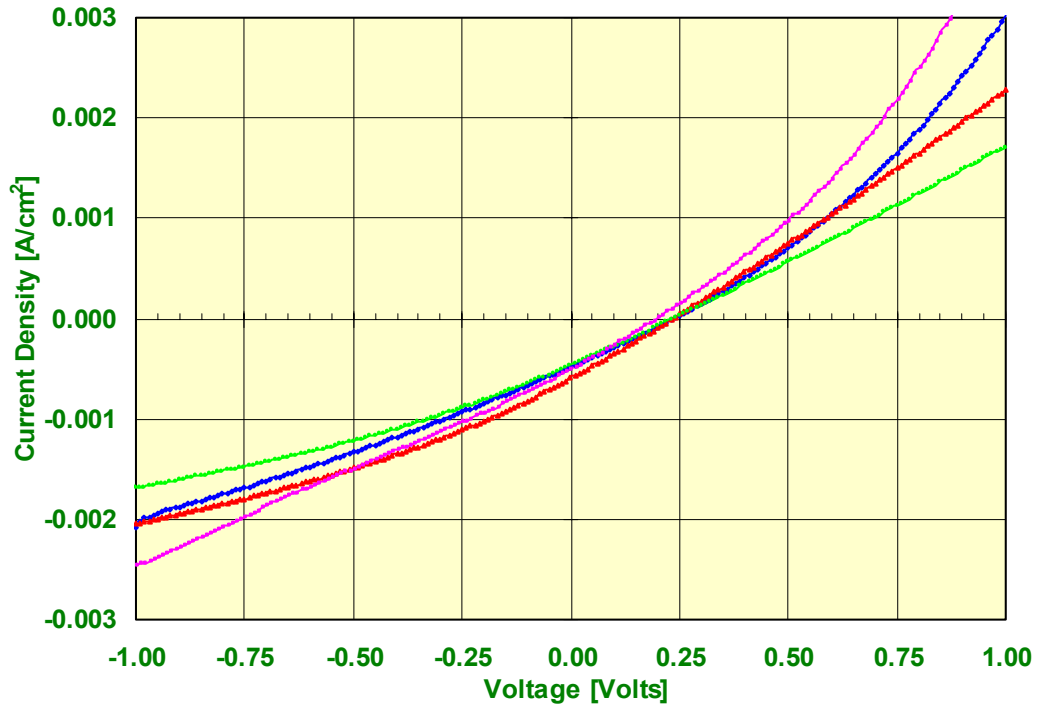


Figure 26. J-V Data for As Deposited SnO₂/CZT Solar Cells

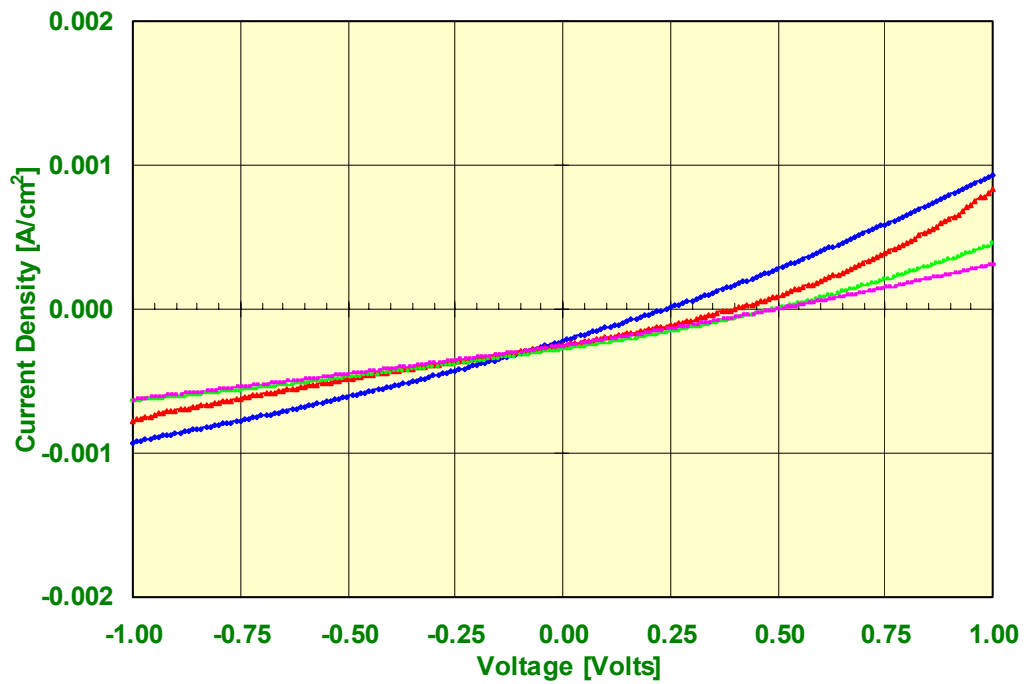


Figure 27. J-V Data for Annealed SnO₂/CZT Solar Cells

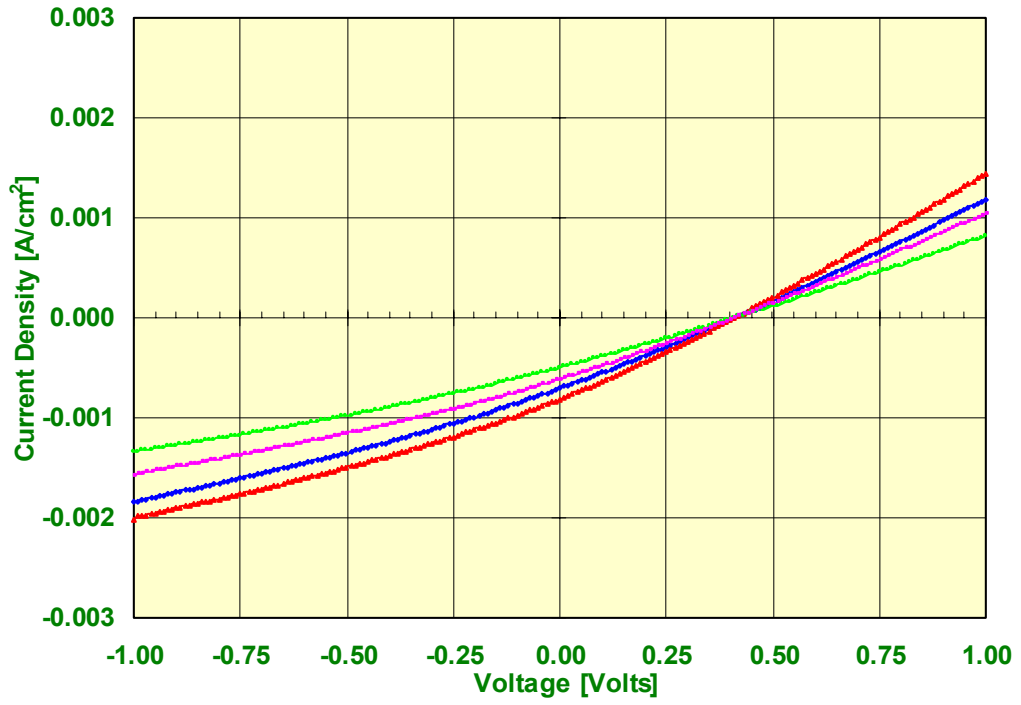


Figure 28. J-V Data for As Deposited SnO₂/CdS/CZT Solar Cells

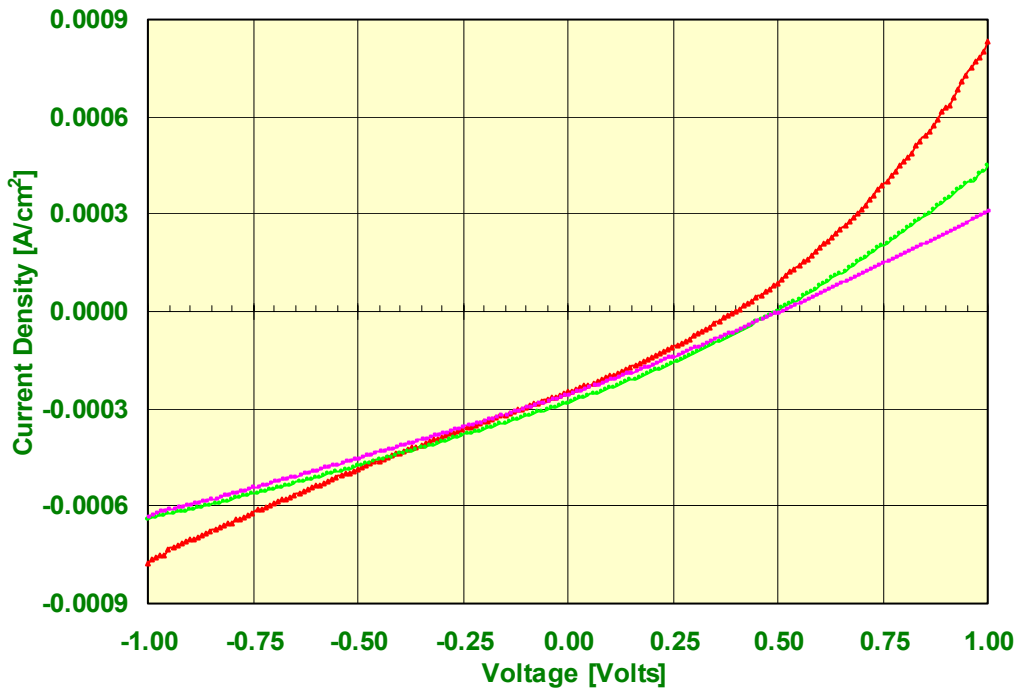


Figure 29. J-V Data for Annealed SnO₂/CdS/CZT Solar Cells

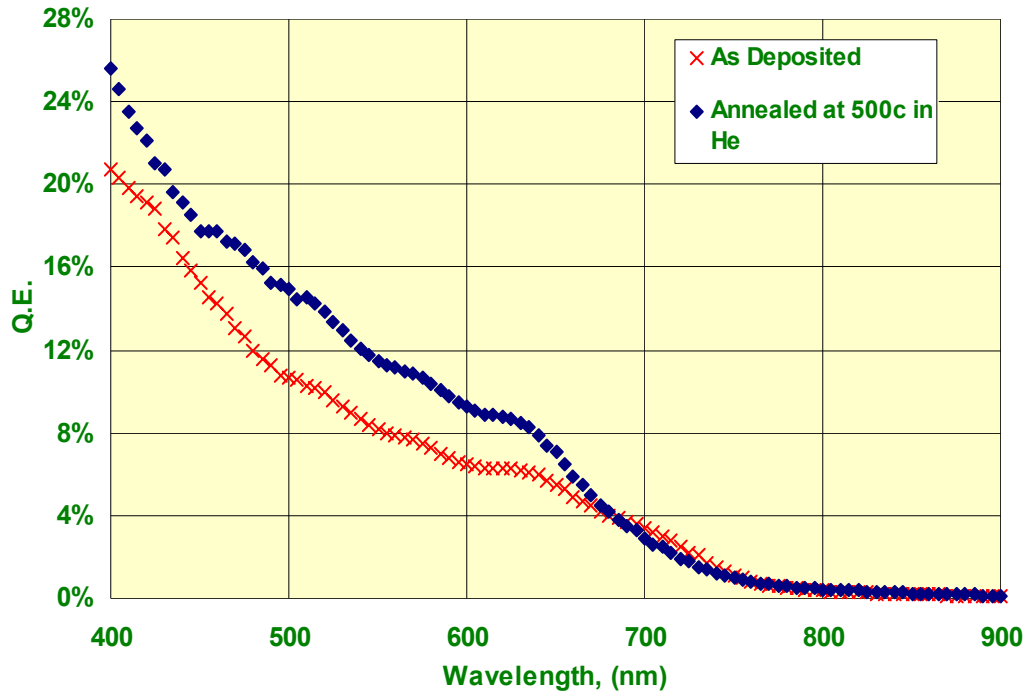


Figure 30. Spectral Response of As Deposited and Annealed SnO₂/CZT Solar Cells

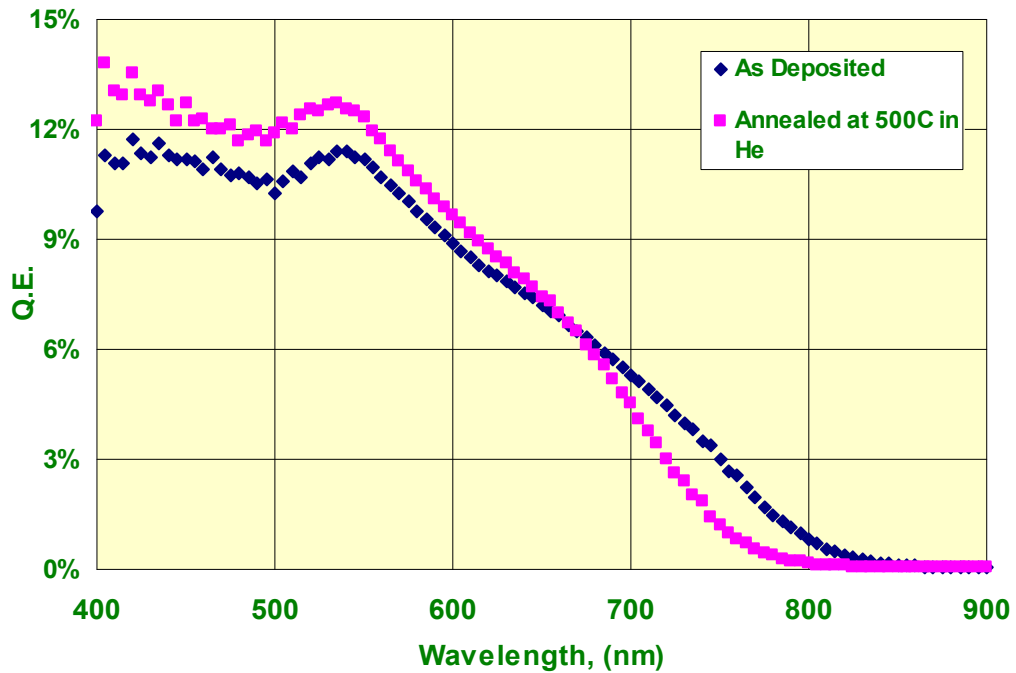


Figure 31. Spectral Response of As Deposited and Annealed SnO₂/CdS/CZT Solar Cells

5.2.4 ZnTe Contact

ZnTe doped with N_2 has been successfully fabricated to obtain good ohmic contacts in CdTe/CdS solar cells [15]. For the CZT devices, ZnTe: N_2 was deposited on CZT before contacting with doped graphite to see if it can improve contact properties and reduce the series resistance of the device. ZnTe was deposited By RF magnetron sputtering in Ar/ N_2 plasma at 200-250 °C to a thickness of 1000-2000 Å. The J-V curves and spectral response are shown below, from which it can be seen that the performance of the devices is similar to non ZnTe devices and there was no significant change in either V_{oc} or J_{sc} from non ZnTe devices.

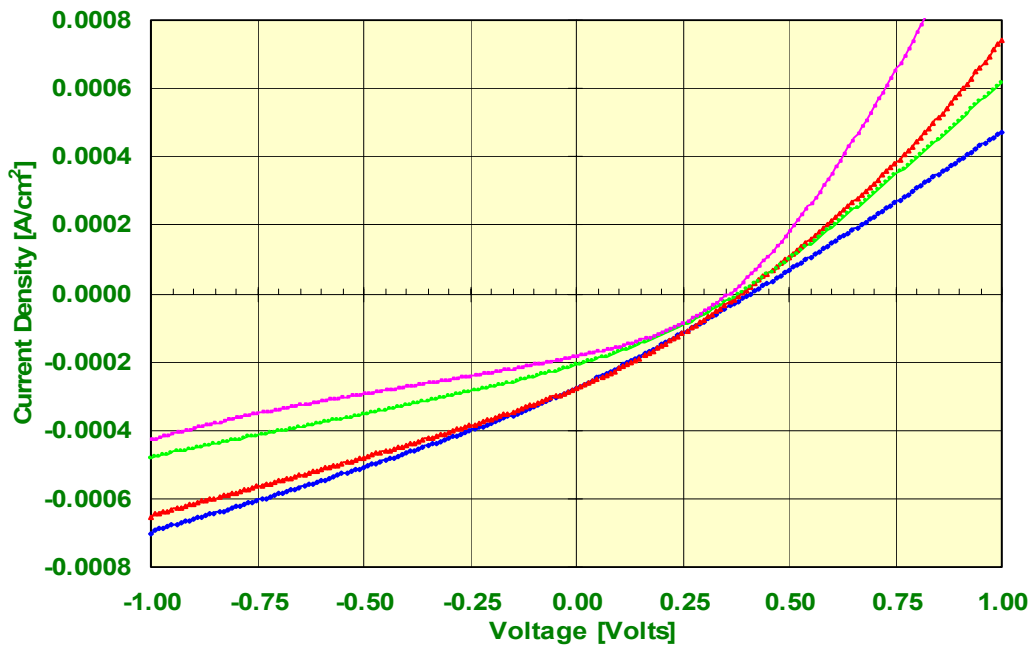


Figure 32. J-V Data for As Deposited $SnO_2/CdS/CZT/ZnTe$ Solar Cells

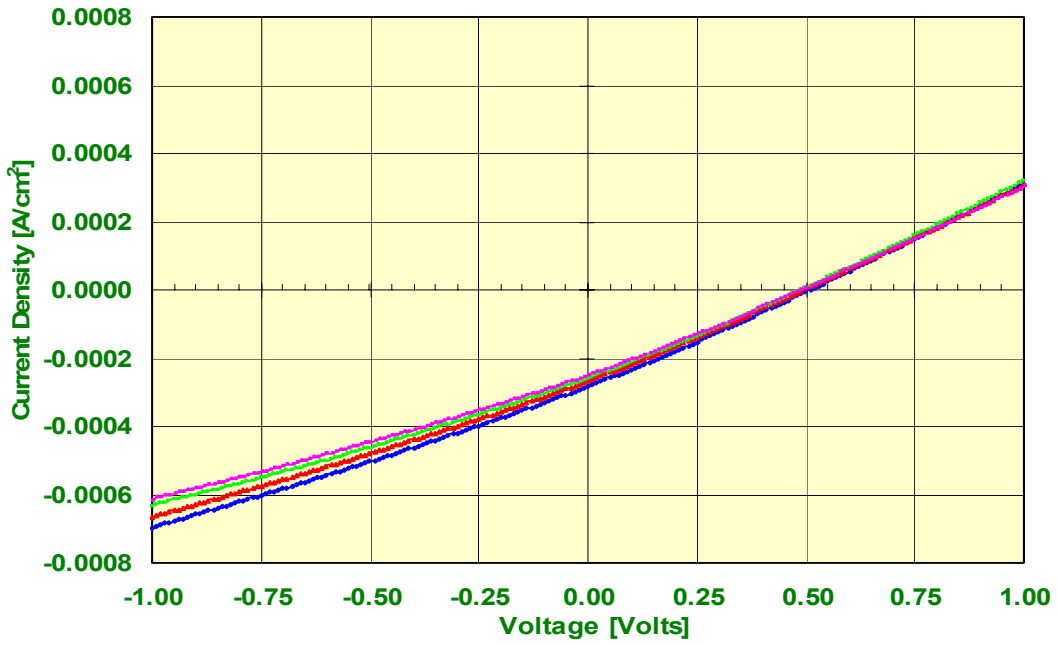


Figure 33. J-V Data for Annealed SnO₂/CdS/CZT/ZnTe Solar Cells

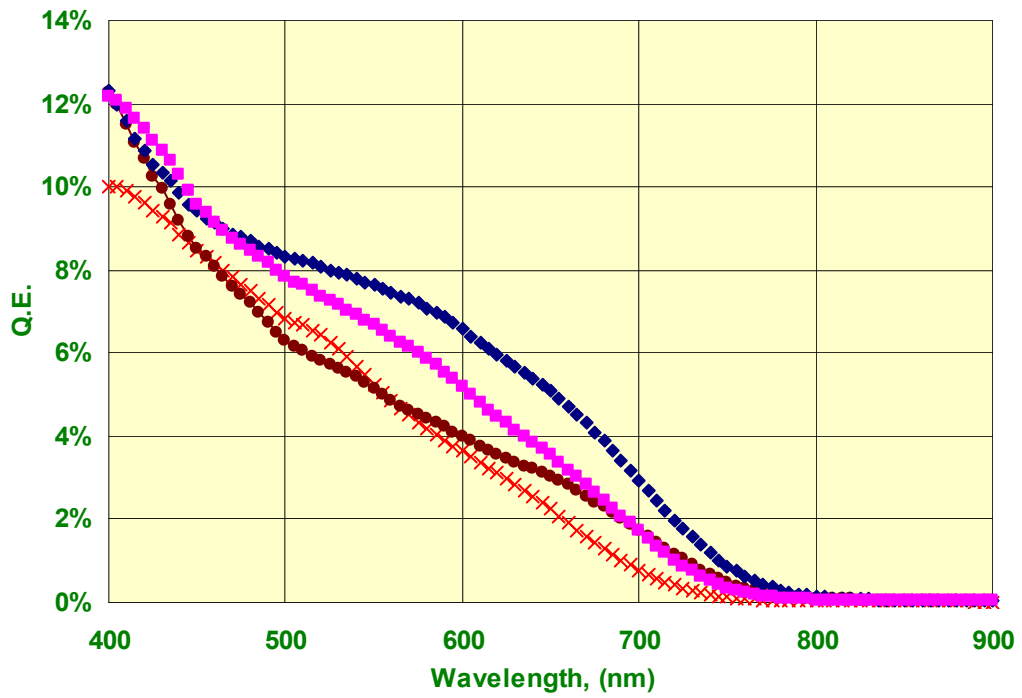


Figure 34. Spectral Response of As Deposited SnO₂/CdS/CZT/ZnTe Solar Cells

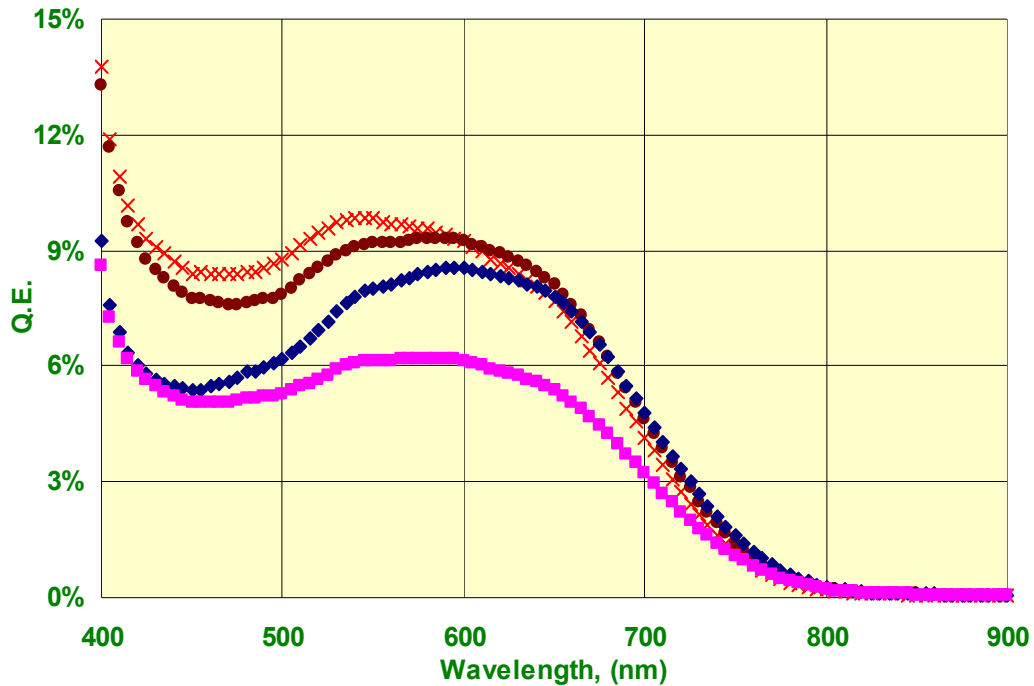


Figure 35. Spectral Response of Annealed SnO₂/CdS/CZT/ZnTe Solar Cells

5.2.5 Post Deposition Treatment on CZT Films

Efforts to utilize chloride treatments on Cd_{1-x}Zn_xTe similar to CdCl₂ treatment on CdTe have not been successful. This is due to chemical reactivity of ZnTe with CdCl₂ resulting in a reaction yielding volatile ZnCl₂ and excess CdTe. However ZnCl₂ will not react appreciably with CdTe which is of great interest [12]. ZnCl₂ treatment was done prior to contacting of the Cd_{1-x}Zn_xTe devices to see if it enhances some of the electronic properties of the Cd_{1-x}Zn_xTe material. Initial experiments were done using ~ 0.2 mol ZnCl₂ solution. CZT deposited on SnO₂/CdS substrates were dipped in the solution for 4-5minutes and these when taken out of the solution were air annealed at 350-400 °C for 10min. This experiment resulted in better currents upto 4.5 mA/cm². This might have been due to removal of ZnTe from the alloy as ZnO and Te [12].

This solution treatment was later replaced by ZnCl_2 vapor treatment. The samples were kept above ZnCl_2 powder placed in a graphite boat and the whole set up was heated in an oven at different temperature so that CZT was exposed to ZnCl_2 vapors. This experiment resulted in better results without causing the loss of Zinc from the CZT bulk as compared to solution treatment. However further studies are needed in order to completely understand the effect of ZnCl_2 on $\text{CdS}/\text{Cd}_{1-x}\text{Zn}_x\text{Te}$ junction and also on electronic properties of $\text{Cd}_{1-x}\text{Zn}_x\text{Te}$ films [26].

5.3 CZT Thin Films on Flexible Polyimide Substrates

After partially optimizing the deposition conditions for CZT on glass substrate, further work was concentrated on fabricating CZT solar cells on flexible substrates. Lightweight flexible polyimide substrates were used for this purpose. Flexible substrates have several advantages over the heavy glass based structures in particular for space applications. Although flexible substrates have advantages over glass substrate, they present certain process challenges as they cannot be exposed to high temperatures and also adhesion of films is one of the issue, which in turn reduce the device performance.

5.3.1 Effect of Temperature on Polyimide Substrate

For this work commercially available KAPTON polyimide was used as a substrate which could withstand upto 400 °C. initial experiments were conducted on polyimide to find the effect of temperature on this substrate. Three substrates were heated at three different temperatures 375 °C, 400 °C, 425 °C and transmission measurements were done on these samples. The only noticeable change was observed for substrate heated at 425 °C which had some physical damage visible to naked eye. The transmission measurements are shown in the figure 37, from which we can see that cutoff is around 450nm which is due to absorption in the polyimide substrate and it can be seen that the transmission of the annealed substrates remains same in most of the region except in the infrared region it increases as the temperature increases, which may just be due to transmission error.

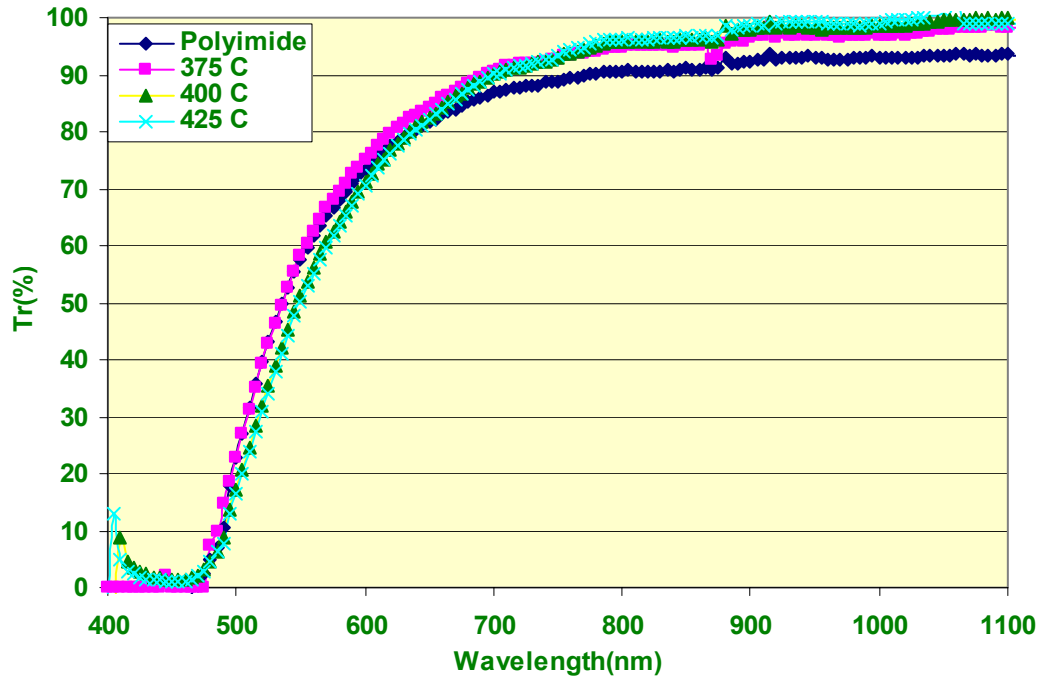


Figure 36. Transmission of Unprocessed and Annealed Polyimide Substrate

5.3.2 TCO Deposition on Polyimide

Indium tin oxide (ITO) films were deposited on polyimide substrates by RF magnetron sputtering at 200-250 °C with Ar and 5% O₂ as plasma source. The total pressure was in the range of 2-3 x10⁻³ torr. The thickness of ITO was ~3000 Å. The sheet resistance of this film was 35 Ω / □. SnO₂ or ZnO were also deposited as bi-layers in different cases on polyimide/ITO substrates in the same chamber without breaking the vacuum to find the adhesion and transmission properties of these films on polyimide. ITO in this case was deposited with Ar only. The thickness of SnO₂ and ZnO was at ~1000 Å and total thickness was maintained at ~3000 Å. The sheet resistance of these films was 7-8 Ω / □. From the transmission response shown in figure 38, it can be seen that ITO deposited with Ar only results in low optical transmission in infrared region which may

be due to free carrier absorption because of highly conductive films. The transmission of ITO deposited with Ar/O₂ plasma source on polyimide is greater than 90% in all the regions which is due to presence of oxygen during deposition which increases the resistivity of films. The adhesion of films on polyimide was good and they did not show any physical damage at 200-250 °C but substrate would curl after heat treatment which was natural for plastics.

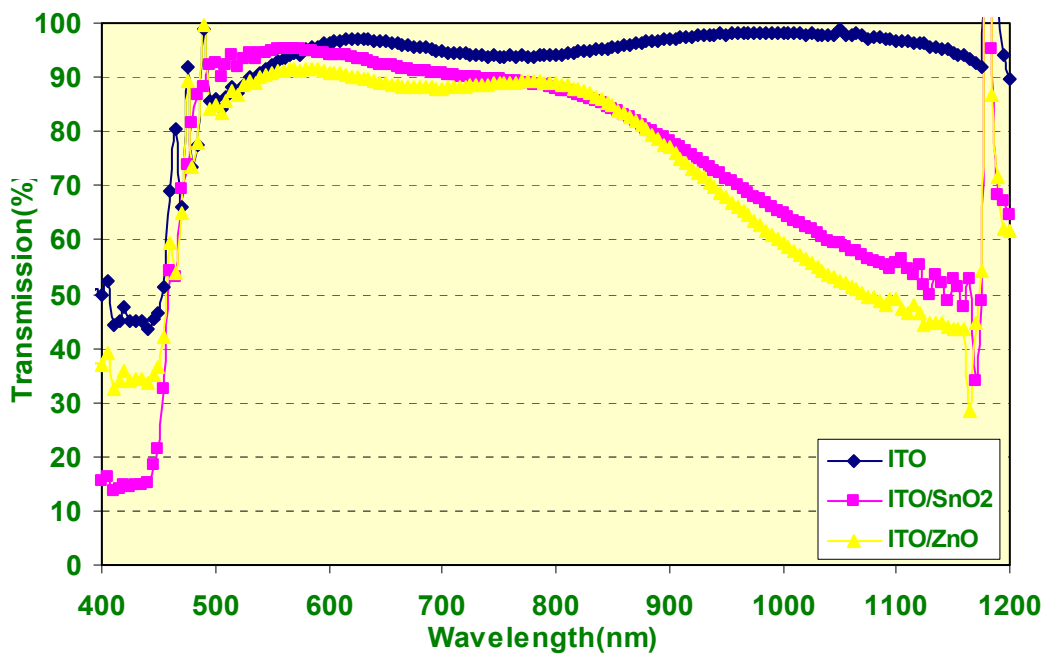


Figure 37. Transmission of ITO, ITO/ZnO and ITO/SnO₂ Films on Polyimide

5.3.3 CZT Films on Polyimide

Cadmium Zinc Telluride (Cd_{1-x}Zn_xTe) was deposited on ITO/CdS, ITO/ZnO/CdS and ITO/SnO₂/CdS substrates. CdS was grown by chemical bath deposition. With CZT problems with adhesion existed which at this time is believed to be due to stress in the CZT films. Further studies are needed to overcome these CZT adhesion problems. However we were able to get better films on some of the substrates. Bandgap,

compositional uniformity and grain structure of CZT on polyimide were studied using XRD and SEM images. With XRD data the zinc concentration in $\text{Cd}_{1-x}\text{Zn}_x\text{Te}$ was determined using the lattice constant relation $a(x)=6.481-0.381x \text{ \AA}$. The value of x was ~ 0.4 corresponding to a bandgap of 1.7eV.

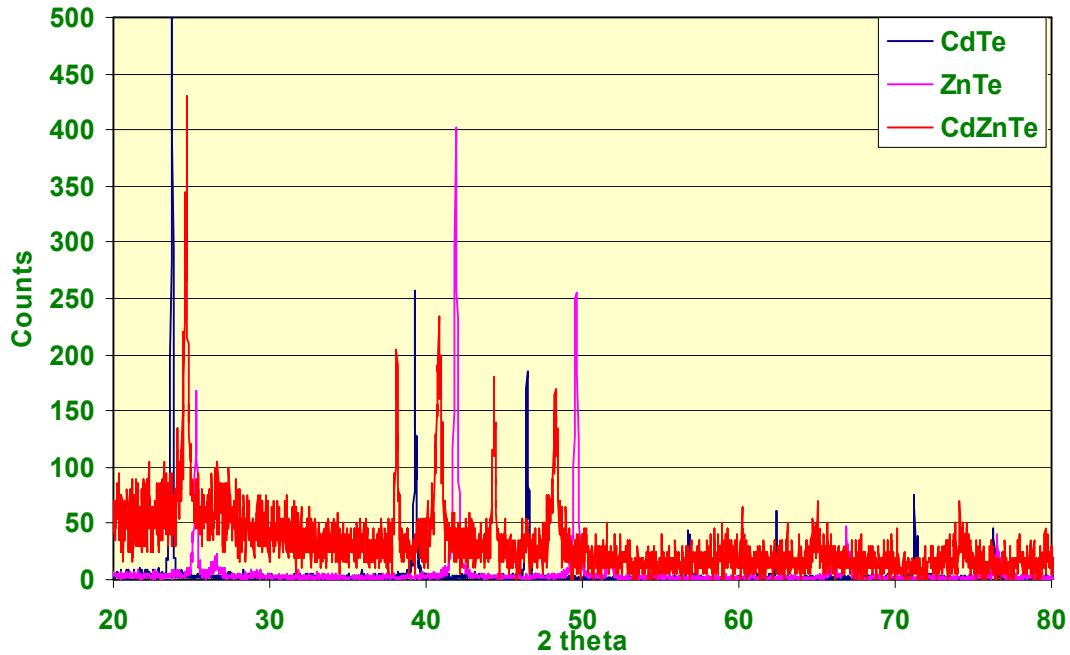


Figure 38. XRD of CZT on Polyimide

From the XRD data we can see that CZT films have preferential (111) orientation. It can also be seen that only peaks corresponding to CZT were observed and no secondary phase can be seen. This may be due to low processing temperature of CZT on polyimide which does not exceed 300°C . Previously CdTe peaks were seen in XRD of CZT on glass substrate which had deposition temperatures up to 400°C . This suggests lower substrate temperatures are favorable for single phase CZT films.

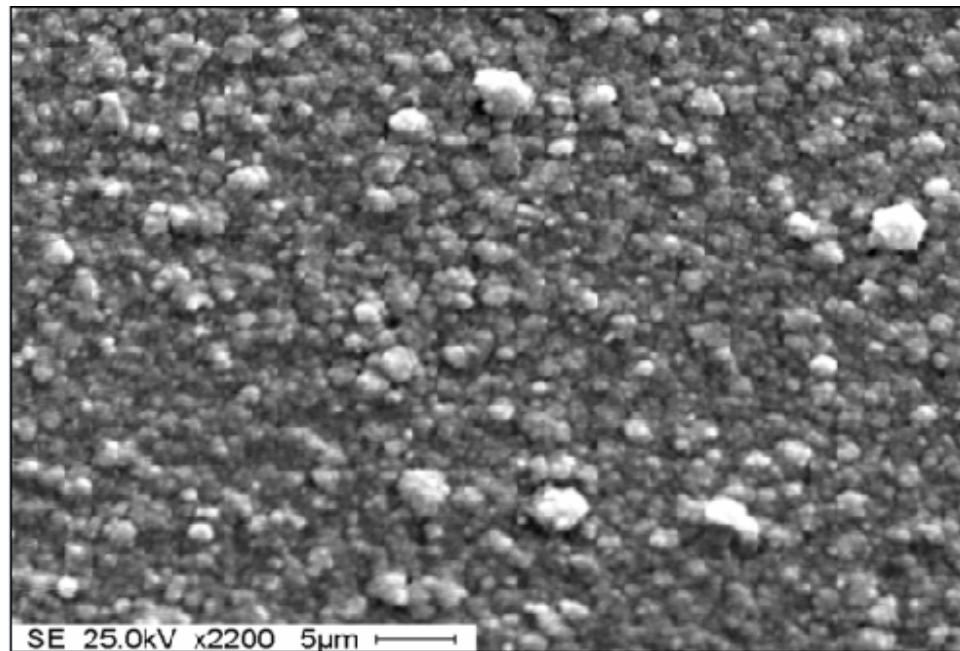
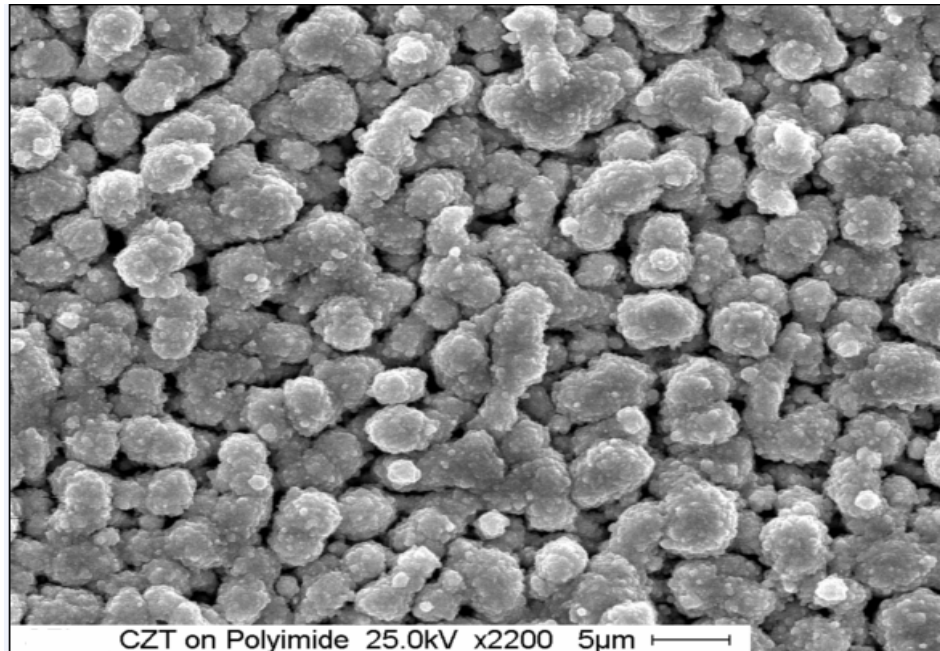


Figure 39. SEM Images of CZT Deposited at 250 °C (Top) and 300 °C (Bottom) on Polyimide Substrate

From the SEM data shown in figure 40, it can be seen that CZT deposited on polyimide at 250 °C is less dense and grain structure looks like clusters of small particles. As the deposition temperature is increased to 300 °C, it can be seen that more closely packed dense films are obtained similar to that on glass substrates which were deposited at 400 °C as shown in figure 19.

CZT solar cells were fabricated on these substrates and were contacted with doped graphite. J-V characteristics for these devices were measured. The cells exhibited V_{oc} 's up to 100mV and currents were less than 1mA/cm² due to excess series resistance. Nevertheless further studies are needed on flexible substrates which provide an interesting alternative to glass substrate in both terrestrial and space applications.

CHAPTER 6

CONCLUSIONS

Cadmium Zinc Telluride films have been successfully deposited by co-sputtering under low temperature conditions on glass and Polyimide substrates. The effects of processing and post deposition heat treatments on CZT films structural and optical properties have been studied and several observations were made.

1) Heat treatments improved crystallinity of the CZT films as indicated by the increased intensity of the XRD peaks. 2) Higher deposition temperature leads to secondary phase in CZT films on glass substrates, however single phase CZT films can be fabricated through lower deposition temperatures (Polyimide). 3) Due to the low processing temperatures used with polyimide substrates CZT films on this type of substrate were less dense with clusters of small particles. 4) Heat treatments did not induce significant grain growth but improved the device performance in terms of V_{oc} and J_{sc} when compared to as-deposited devices.

The influence of N_2 during the deposition of $Cd_{1-x}Zn_xTe$ on the device performance was studied. Films deposited with Ar and 50% N_2 as partial pressure exhibited better performance. V_{oc} 's up to 670 mV and J_{sc} 's up to 2.5 mA/cm² were obtained with these deposition conditions. The use of ZnTe: N_2 as the back contact did not improve the performance of the devices to large extent.

Post deposition $ZnCl_2$ treatment was done on $Cd_{1-x}Zn_xTe$ films similar to $CdCl_2$ treatment in high efficiency CdTe solar cells. $ZnCl_2$ Vapor treatment did improve the device performance to certain extent with out change in bulk composition, but further studies are needed in order to completely understand the effect of $ZnCl_2$ on $Cd_{1-x}Zn_xTe$ films.

$Cd_{1-x}Zn_xTe$ solar cells were fabricated for the first time on flexible polyimide substrates. Commercially available KAPTON polyimide was used for our experiments which could withstand up to $400\text{ }^\circ\text{C}$. Devices made out of these films had low V_{oc} 's and J_{sc} 's due to high series resistance. Further studies are needed to completely study the device performance on these flexible polyimide substrates.

The low currents in the CZT devices can be attributed to low collection in long wavelength region. This may be due to poor interface/junction properties or poor electronic properties of CZT.

REFERENCES

- [1] "International Energy Outlook 2003", Energy Information Administration, US Department of Energy, 2003. [<http://www.eia.doe.gov/oiaf/ieo/index.html>]
- [2] C.Gary, B.Lynn, A.Rick, "Photovoltaic Fundamentals", Solar Energy Research Institute, Springfield, VA : Available from National Technical Information Service, 1991.
- [3] "Photovoltaic Energy Program Overview", US Department of Energy, 2000. [<http://www.nrel.gov/docs/fy01osti/28976.pdf>].
- [4] Photovoltaics Overview 2001, Office of Solar Energy technologies, US department of Energy, 2001. [<http://www.nrel.gov/docs/fy02osti/30729.pdf>].
- [5] P.Selvaraj, "Effect of Cadmium Chloride Treatment on CdS-CdTe Solar Cells", Master's Thesis, University of South Florida, Tampa, 1999.
- [6] C.E. Backus "Solar cells", IEEE press 1976, p.24.
- [7] A. Rohatgi, R. Sudarshanan, S.A.Ringel, "Wide Bandgap Thin Film Solar Cells from CdTe Alloys", 20th IEEE Photovoltaic Specialists Conference, pp.1477-1481, 1988.
- [8] J.S.Britt, "II-VI Compound Thin Films by MOCVD for Tandem Solar Cells", Ph.D Dissertation, University of South Florida, Tampa, 1992.
- [9] L.Zhihong, H.Xiaokang and W.B.Berry, " Temperature dependence on the Energy Gap Selection in Two Cell, Four Terminal Tandem Solar Cell design" 22nd IEEE Photovoltaic Specialists Conference, pp.323-328.
- [10] W.Ma, T.Horiuchi, C.C.Lim, K.Goda, H.Okamoto, Y.Hamakawa, " An Optimum Design of a a-Si/poly-Si Tandem Solar Cell", 23rd IEEE Photovoltaic Specialists Conference, pp.833-838.
- [11] C.S.Ferekides and D.L.Morel, " Development of II-VI-based High Performance High Bandgap Device for Thin Film Tandem Solar Cells", National Center for Photovoltaics Program Review Meeting, Lakewood, CO, Oct. 14-17, 2001.
- [12] B.E.Mccandless, " Cadmium Zinc Telluride Films for Wide Bandgap Solar Cells", 29th IEEE Photovoltaic Specialists Conference, pp.488-491, 2002.

- [13] A.Burger, H.Chen, K.Chattopadhyay, D.Shi, S.H.Morgan, W.E.Collins, R.B.Jones, "Characterization of Metal Contacts on and Surfaces of Cadmium Zinc Telluride", Nuclear Instruments and methods in Physics Research, pp.8-13,1999.
- [14] Linjun wang, wenbin sang, Weimin Shi, Yongbiao Quin, jiahua Min, Donghua Liu, Yiben Xia, "Electrical Properties of Contacts on P-type Cd_{0.8}Zn_{0.2}Te Crystal Surfaces", Nuclear Instruments and methods in Physics Research, pp.581-585, 2000.
- [15] T.A.Gessert, P.Sheldon, X.Li, D.Dunlavy, D.Niles, "Studies of ZnTe Back Contacts to CdS/CdTe Solar Cells", IEEE 26th Photovoltaic Specialists Conference, pp.419-422,1997.
- [16] Makhratchev, K.J.Price, D.A.simmons, J.Drayton, A.Gupta, R.G.Bohnan, A.D.Compaan, "ZnTe:N Back Contacts to CdS/CdTe Solar Cells", IEEE 28th Photovoltaic Specialists Conference, pp.475-478, 2000.
- [17] M.Xavier, T.Gerald., V.P.Singh, J.C.McClure, S.Velumani, R.Mathew, P.J.Sebastian, "Development of CdTe Thin Films on Flexible Substrates", Solar Energy Materials and Solar Cells, Vol 76, pp.293-303, 2002.
- [18] A.N.Tiwari, A. Romeo, D.Baetzner and H.Zogg, "Flexible CdTe Solar Cells on Polymer Films", Progress in Photovoltaics: Research and Applications , pp.211-215, 2001.
- [19] J.Herrero,C.Guillen, "Transparent Films on Polymers for Photovoltaic Applications", Surface Engineering ,Surface Instrumentation and Vacuum Technology, Vol 67, pp.611-616, 2002.
- [20] S.Wiedman, R. Butcher, J.Fogleboch, J.Muha, R.G.Wendt, M.E.Beck, J.S.Britt, "CIGS Processing on Flexible Polyimide Substrates", National Center for Photovoltaics Program Review Meeting, Colorado, Oct 15,2001.
- [21] A.N.Tiwari, A.Romeo, D.Baetzner and H.Zogg, "Influence of Proton Irradiation and Development of Flexible CdTe Solar Cells on Polyimide", Proceedings of 2001 Material Research Society Spring Meeting, San Francisco CA, USA, 16-20 April 2001.
- [22] S.N.Alamri and A.W.Brinkman, "The Effect of Transparent Conductive Oxide on the Performance of Thin Film CdS/CdTe Solar Cells", J. Phys. D : Appl Phys.33, L1-L4, 2000.
- [23] T.L.Chu, S.S.Chu, C.S.Ferekides, C.Q.Wu, J.Britt, C.Wang,"High Efficiency CdS/CdTe Solar Cells from Solution Grown CdS Films", IEEE 22nd Photovoltaic Specialists Conference, Vol 2, pp.952-956, 1991.
- [24] S.Tatarenko, T.Baron, A.Arnoult, J.Cibert, M.Grun, A.Haury, Y.Merle, A.Wasiela, K.Saminadayar, "Nitrogen Doping of Te Based II-VI Compounds", Journal of Crystal Growth, pp.682-687,1997.

- [25] D.N.Marinskiy, "Cadmium Sulphide Thin Films Deposited by Close Spaced Sublimation and CdS/CdTe Solar Cells", Ph.D. Dissertation, University of South Florida, Tampa, 1998.
- [26] These results are from the work of my colleague S.Subramanian and will be included in his thesis to be submitted in summer 2004 to Electrical Engineering Department of University of south Florida.